University of Illinois at Urbana-Champaign

ACRC

Air Conditioning and Refrigeration Center A National Science Foundation/University Cooperative Research Center

Tribological Studies on Scuffing Due to the Influence of Carbon Dioxide Used as a Refrigerant in Compressors

N. G. Demas, A. A. Polycarpou, and T. F. Conry

ACRC TR-222 December 2003

For additional information:

Air Conditioning and Refrigeration Center
University of Illinois
Mechanical & Industrial Engineering Dept.
1206 West Green Street
Urbana, IL 61801

(217) 333-3115

Prepared as part of ACRC Project #133
Tribological Studies on Scuffing Due to the Influence of CO_2 Used as a Refrigerant in Compressors
A. A. Polycarpou and T. F. Conry, Principal Investigators

The Air Conditioning and Refrigeration Center was founded in 1988 with a grant from the estate of Richard W. Kritzer, the founder of Peerless of America Inc. A State of Illinois Technology Challenge Grant helped build the laboratory facilities. The ACRC receives continuing support from the Richard W. Kritzer Endowment and the National Science Foundation. The following organizations have also become sponsors of the Center.

Alcan Aluminum Corporation
Amana Refrigeration, Inc.
Arçelik A. S.
Behr GmbH and Co.
Carrier Corporation
Copeland Corporation
Daikin Industries, Ltd.
Delphi Harrison Thermal Systems
Embraco S. A.
General Motors Corporation
Hill PHOENIX
Honeywell, Inc.
Hydro Aluminum Adrian, Inc.
Ingersoll-Rand Company
Lennox International, Inc.
LG Electronics, Inc.
Modine Manufacturing Co.
Parker Hannifin Corporation
Peerless of America, Inc.
Samsung Electronics Co., Ltd.
Sanyo Electric Co., Ltd.
Tecumseh Products Company
Trane
Visteon Automotive Systems
Wieland-Werke, AG
Wolverine Tube, Inc.

For additional information:

Air Conditioning & Refrigeration Center
Mechanical & Industrial Engineering Dept.
University of Illinois
1206 West Green Street
Urbana, IL 61801

217 333 3115

Abstract

The refrigeration and air conditioning industry has expressed a great interest in the use of carbon dioxide (CO_2) as a refrigerant. CO_2 is anticipated to replace HFC refrigerants, which are known to have a negative effect on the environment. The reason behind the interest in CO_2 is the fact that it is a natural refrigerant, thus environmentally acceptable. Of course, such a replacement raises concerns regarding design criteria and performance due to the different thermodynamic properties of CO_2 and the very different range of pressures required for the CO_2 refrigeration cycle.

So far, work related to CO_2 has been done from a thermodynamics point of view and researchers have made significant progress developing automotive and portable air-conditioning systems that use the environmentally friendly carbon dioxide as a refrigerant. The purpose of this work is to develop an understanding of how CO_2 plays a role from a tribology standpoint. More specifically, the goal of this work is to gain an understanding on how CO_2 influences friction, lubrication, wear and scuffing of tribological pairs used in compressors.

Work in the area of tribology related to CO_2 is very limited. Preliminary work by Cusano and coworkers showed that consistent data for tests using CO_2 could not be acquired nor could a satisfactory explanation be offered for the inconsistency. Their results triggered the initiation of the work presented here. In this first attempt to understand the tribological behavior of CO_2 several problems were encountered. During this work we noted that its behavior, unlike conventional refrigerants, could not always be predicted. We believe that this can be attributed to the thermodynamic properties of CO_2, which cannot be ignored when studying its tribological behavior. Thermodynamic Properties such as miscibility are very important when tribological testing is performed. A limiting factor with our tester was that it was not designed for CO_2 testing, but for other conventional refrigerants and therefore made previously developed testing protocols non-applicable with CO_2. Through a different approach and some modifications to our tester we were able to establish a protocol for testing under the presence of CO_2. CO_2 was then compared to R134a and the experimental results showed that it performs equally well.

Table of Contents

List of Figures

Page

List of Tables

Page

Chapter 1. Carbon Dioxide (CO_2)

1.1 Tribology of CO_2 Compressors

Work in the area of tribology related to CO_2 is very limited. Most of the work related to CO_2 has focused on the development of the main components for the required transcritical CO_2 cycle such as the compressor and the expansion device but always with a focus on the thermodynamic aspect. Most of this development is at a prototype stage design and includes scroll compressors (Hagita et al., 2002), hermetic compressors (Suss, 2000), hermetic swing compressors (Ohkawa, 2002), and piston-cylinder expansion devices (Baek et al., 2002). Researchers have also focused on the aspect of lubrication in refrigeration compressors using CO_2 (Johnson, 1998). Some aspects of their work are related to tribology in the sense that they involve studies on lubrication of bearings in a scroll compressor. However, material examination of surfaces in compressors that use CO_2, comparative studies on friction, wear, lubrication, scuffing or on the effects of the environmental conditions using different refrigerants is absent from the open literature as of this date.

Preliminary work by Cusano and Stokes (1999) showed that testing with CO_2 can be an intricate task. Their preliminary results showed large variability in the scuffing load that could not be adequately explained. Such task, dealing with a comparative study of refrigerants and their tribological performance, has not been undertaken before which makes the work of tribology related to CO_2 a building block of significant importance.

1.2 General Background Related to CO_2

Carbon dioxide (CO_2) was first recognized by Jan Baptista van Helmont (1580-1644) who detected it in the products of both fermentation and charcoal burning. It occurs in the products of combustion of all carbonaceous fuels and can be recovered from them in a variety of ways. It is present in the atmosphere in small quantities being uniformly distributed over the earth's surface at a concentration of about 0.033% or 330 parts per million. Because the concentration of CO_2 in the atmosphere is very low, it is not practical to obtain the gas by extracting it from air. Most commercial CO_2 is recovered as a by-product of other processes, such as the production of ethanol by fermentation and the manufacture of ammonia, from flue gases by absorption processes, and furnace operations. Some CO_2 is obtained from the combustion of coke or other carbon-containing fuels. CO_2 is also a product of animal metabolism and is important in the life cycles of both animals and plants. It finds uses in solid, liquid and gaseous form in a variety of industrial applications such as welding, beverage carbonation and in fire extinguishers.

CO_2 dissolves readily in many liquids. Under normal temperature and pressure conditions, CO_2 gas dissolves in an equal volume of water. The greater the pressure, the more CO_2 a liquid can hold in solution, but excess CO_2 remains dissolved only as pressure is applied. When released, excess CO_2 escapes in the effervescent bubbling characteristics of uncapped soft drinks. CO_2 is not very reactive at normal temperatures. It does however form carbonic acid (H_2CO_3) in aqueous solutions, which is a weak and unstable acid that tends to revert to CO_2 and H_2O. H_2CO_3 undergoes the typical reactions of a weak acid to form salts and esters. CO_2 is very stable at normal temperatures, but forms CO and O_2 when heated above 1700°C.

CO_2 can be reduced by several methods, the most common being its reaction with hydrogen. It can also be reduced with hydrocarbons and carbon at elevated temperatures. CO_2 will react with ammonia to form ammonium carbonate, which is used as the first stage of urea manufacture. CO_2 is a normal constituent of exhaled air but high

concentrations of the gas are hazardous. Five percent of CO_2 by volume in air increases the breathing rate and prolonged exposure to volumes greater than 5% can cause unconsciousness and/or death. Since carbon dioxide is almost 53% heavier than air with a specific gravity of 1.53 at 21°C, it will settle to the bottom of a room or container and displace air. In addition to being a component of the atmosphere, CO_2 also dissolves in the water of the oceans. The most important properties of carbon dioxide have been summarized in Table A.1 (ASHRAE, 1969) in the Appendix.

1.3 CO_2 Phase Diagram

CO_2 can exist in three states: gas, liquid and solid. At normal temperatures and pressures, CO_2 is a colorless gas. When compressed and cooled to the proper temperature, the gas turns into a liquid. The liquid in turn can be converted into solid known as dry ice. The dry ice, on absorbing heat, returns to its natural gaseous state. There are two interesting points one can observe on the phase diagram of CO_2: the triple point and the critical point.

1.3.1 Triple Point

The triple point is the point where CO_2 can exist simultaneously in its three states as gas, liquid and solid. The pressure and temperature that correspond to the triple point are 75.35 psi and -56.6°C (-69.88°F), respectively. If the pressure is reduced from the triple point, the liquid flashes to solid and gas. If the temperature is reduced, the liquid freezes. If the temperature is increased, the liquid boils, which generates gas. These phase changes can be seen in Figure 1.1.

1.3.2 Critical Point

Above the critical temperature point of 31.04°C (87.87°F) it is impossible to liquefy the gas by increasing the pressure above the corresponding critical pressure of 1069.96 psi. This is evident in Figure 1.1 since the liquid-gas line stops right at the critical point. At temperatures higher than this point there can no longer be two phases. There is only a single phase, which is a very dense gas often called a supercritical fluid.

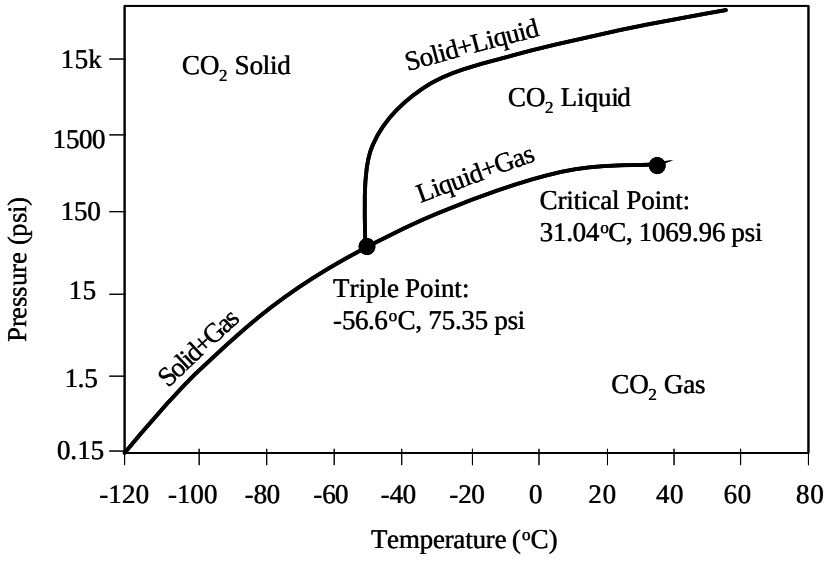

Figure 1.1 - Phase Diagram for CO_2

1.3.3 CO_2 as a Liquid

CO_2 is most commonly stored and transported as a liquid. CO_2 does not exist in liquid form at atmospheric pressure at any temperature. The pressure-temperature phase diagram of Figure 1.1 shows that liquid CO_2 at 21°C (70°F) requires a pressure of 441 psi. The lowest pressure at which liquid CO_2 exists is at the triple point at 75.35 psi and that is the minimum pressure required in order to remain a liquid.

1.3.4 CO_2 as a Solid

The normal temperature of solid CO_2 (dry ice) is -78.45°C (-109.21°F). At ambient temperature and atmospheric pressure, the solid sublimes slowly, leaving no residue, as it changes directly back to gaseous form.

1.4 CO_2 Used as Refrigerant

In recent years, the refrigeration industry has shown a great deal of interest in the use of CO_2 as a refrigerant with the potential to replace commonly used refrigerants. CO_2 is a proven viable refrigerant. It has been used in the past as a refrigerant, but the high pressures at which CO_2 systems have to be operated at and the low critical temperature limited its use in refrigeration systems. However, recent advances in compressor designs and prototype systems have demonstrated significant improvements in energy efficiency compared to R134a (Pettersen, 1997).

For nearly six decades, chlorofluorocarbon refrigerants (CFCs) have been used for as solvents, aerosol propellants and refrigerants. CFCs are long-lived compounds which, when released, rise to the stratosphere where they are decomposed by UV light and form free chlorine. The chlorine released reacts with the earth's ozone. Chlorine atoms in the stratosphere are very reactive and each one may destroy hundreds of thousands of molecules of ozone before removed. Their harmful effect on the Earth's protective ozone layer was first published by Rowland and Molina in 1974. Subsequently, the ozone hole over the Antarctic was discovered and heightened world attention that led to the Montreal Protocol of 1989. Over the same period, it was discovered that CFCs also contributed significantly to the world's greenhouse warming problem. The global warming potential (GWP) of the CFC refrigerant R12 is 7100 times that of carbon dioxide over twenty years (Lorentzen, 1995). The GWP represents how much a given mass of a chemical contributes to global warming over a given time period compared to the same mass of carbon dioxide whose GWP is defined as 1.0. The response of the chemical industry was to develop new synthetic refrigerants without the harmful chlorine atoms, which cause ozone depletion. These are known as hydrofluorocarbons (HFCs), of which the best known is R134a. However, their high global warming potential is also significant, though less than that of CFCs as it can be seen in Table 1.1.

Carbon dioxide on the other hand, has no ozone depleting potential and a negligible direct global warning effect as seen on Table 1.1.

Table 1.1 - Characteristics of CO_2 (Lorentzen, 1995)

	Ozone Depleting Potential	Global Warming Potential (20 years integration time)	Critical Temperature (°C)
CO_2	0	1	31.1
R134a	0	3100	101.2
R22	0.05	4100	96.1
R12	1.0	7100	112.0

CO_2 is non-flammable, chemically inactive, nontoxic and inexpensive. Due to these properties, along with the fact that it is a natural refrigerant and therefore environmentally acceptable, the refrigeration and air conditioning industry has expressed a great interest in its use and is anticipated to replace HFC refrigerants. However, such a replacement raises concerns regarding design criteria and performance and safety due to the different thermodynamic properties of CO_2 and the very different range of pressures required for the CO_2 refrigeration cycle for typical applications in refrigeration. The difference in the range of pressures between CO_2, R134a and R22 can be seen in Figure 1.2.

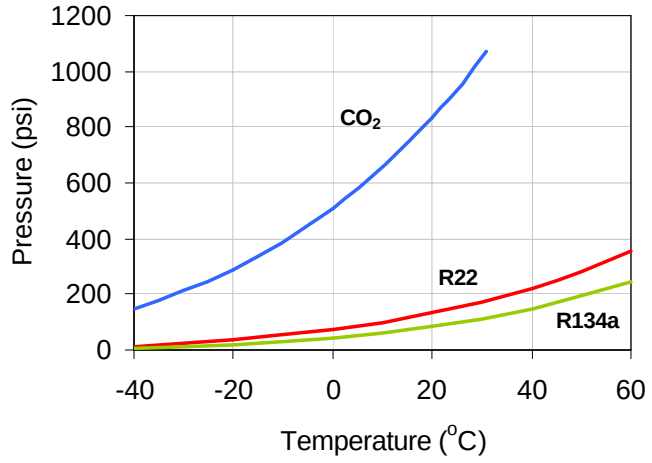

Figure 1.2 - CO_2/R134a/R22 Comparison of Pressure Levels

A typical transcritical cycle for CO_2 is shown in Figure 1.3. Unlike R134a, the CO_2 gas is compressed well above the critical point and the heat rejection process takes place in the critical region.

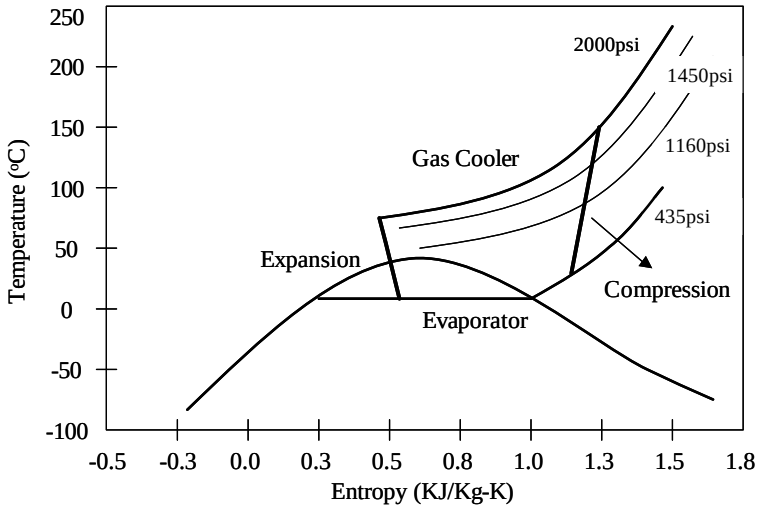

Figure 1.3 - Typical Transcritical CO_2 Cycle for Refrigeration

Typical operating conditions for CO_2 and R134a are shown in Figure 1.4. Both are plotted on the same graph for contrast. The discharge pressure with CO_2 is extremely high and the critical temperature at 31°C (1070 psi) is very low. For single stage systems this requires transcritical-operating conditions with discharge pressures

greater than 1500 psi. Also, the pressure of CO_2 is about 10 times that of R134a, so when designing CO_2 compressors it is vital to solve the problems that arise by the need for higher loads of the sliding parts and the differential pressures of the sealing parts (Hagita et al., 2002). Another major problem with CO_2 is that its thermodynamic cycle characteristics result in system coefficients of performance (COP) that are typically lower than HFC vapor compression systems (Brown et al., 2002).

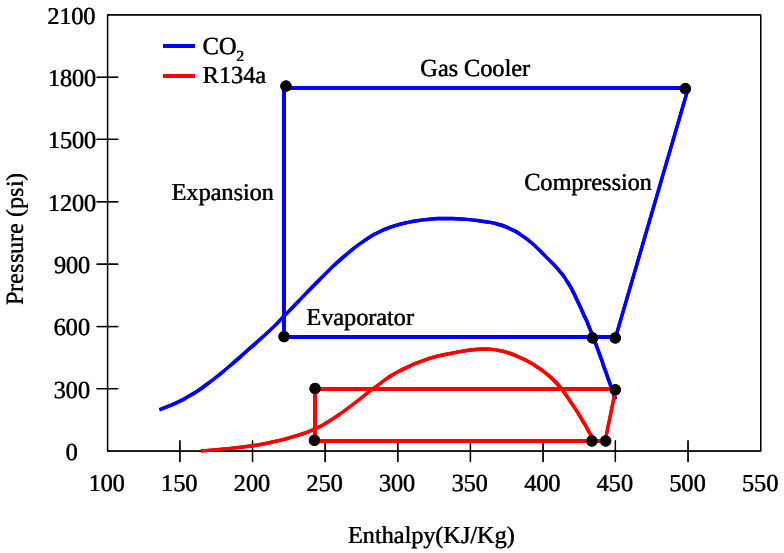

Figure 1.4 - Typical operating conditions for CO_2 and R134a

So, at a glance it may seem that CO_2 is in some ways inferior to other refrigerants. However, due to its high volumetric capacity and the elimination of recovery and recycling equipment and the subsequent procedures, carbon dioxide has received much attention for several applications.

1.5 Miscibility of Lubricants in CO_2

The role of lubricants in refrigeration compressors is to reduce friction and prevent wear. Lubricant chemistry, density, miscibility and solubility with CO_2 are some very important parameters one would have to take into consideration. A wide range of optimized lubricants is available for different refrigerants. Lubricant options allow the selection of particular performance characteristics appropriate to the system. Therefore, the selection of a lubricant for a CO_2 compressor is of great importance since it can have a major impact on the performance and reliability of the system. It has been suggested that lubrication of CO_2 compressors is difficult due to the high operating pressure of CO_2. Solubility is also of particular interest, however, the major concern is miscibility of different lubricants in CO_2. A refrigerant and lubricant are described as miscible when they form one single liquid phase. On the other hand solubility can be thought of as when the refrigerant contains a proportion of the lubricant and vice-versa. An immiscible mixture of lubricant and refrigerant can still possess a degree of mutual solubility. Modern synthetic lubricants can be designed to interact with refrigerants in specific ways. The most commonly used lubricants with CO_2 as far as experience or compatibility is concerned are polyol ester (POE), and polyalkylene glycol (PAG) lubricants. In Figure 1.5 we can see a miscibility chart (Seeton, 2000) with these lubricants.

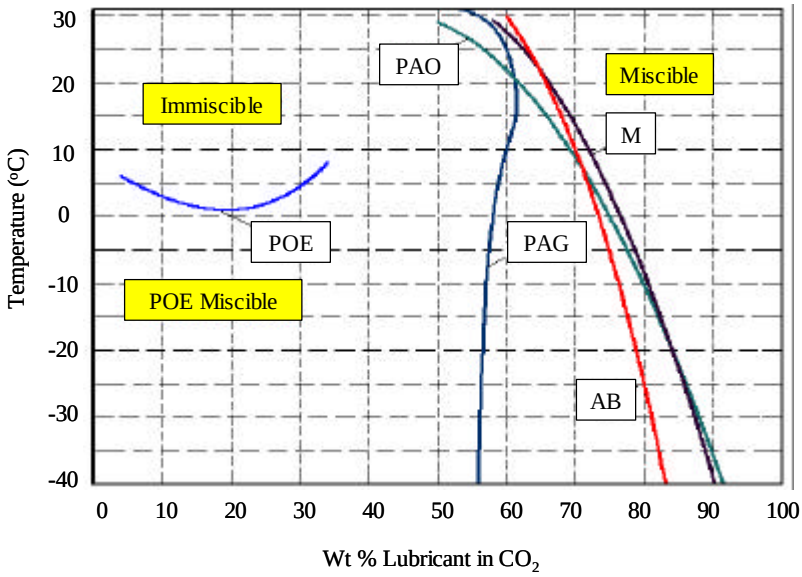

Figure 1.5 - Miscibility Chart of Different Lubricants in CO_2 (Seeton, 2000)

POEs have wide market acceptance with HFC refrigerants. Applications include appliance, refrigeration and air-conditioning. Ester chemistry allows the use of numerous alcohols and acids that can be combined to make esters with desired properties (Randles, 1999). As a result, POE-based refrigeration lubricants with structures designed to control miscibility and solubility and other properties have been developed. POEs have a high degree of solubility and miscibility with CO_2.

PAGs are polymers of alkylene glycols. Typically, they are polymers of ethylene oxide, propylene oxide, butylenes oxide or copolymers of the above. The chemical structure of PAGs can also be varied to give desired miscibility and solubility with the HFC refrigerants. This is often achieved by varying the ratios of ethylene oxide and propylene oxide in the synthesis process (Matlock et al., 1999). Currently, PAG is the lubricant of choice in most R-134a automobile A/C systems. In addition, they are good candidates for use in CO_2 systems.

1.6 Thesis Outline

In Chapter 2, the High Pressure Tribometer (HPT) used for the experimental tribological testing, and the experimental setups for all the different types of tests performed in this work have been described. In Chapter 3, the motivation for performing the different types of tests has been presented along with the results and discussion of our tests. The main point of this chapter is the fact that a test protocol for testing under refrigerant environments was established that led to different series of tests that make comparative studies possible and allow us to obtain qualitative results about the behavior and performance of CO_2 under numerous operating conditions. Chapter 4 contains experimental techniques and uncertainties about some of the types of tests that were performed. Due to some inconsistencies in sample preparation some of the results did not exhibit repeatability. We offer some criticism as well as an explanation to why we believe we have presented representative results from the series of tests that were not repeatable. Finally in Chapter 5 some conclusions and recommendations have been presented. Under the presence of PAG lubricant and the same environmental conditions, CO_2 and R134a performed almost identically. Furthermore, in the absence of lubricant, CO_2 performed very similar to R134a.

Chapter 2. High Pressure Tribometer (HPT) and Experimental Tribological Testing

2.1 Introduction

The High Pressure Tribometer (HPT) is an instrument used to run wear and friction tests using a lower stationary sample in contact with an upper rotating sample. It accurately simulates the environmental conditions found in a typical air conditioning compressor. A photograph of the HPT and a schematic of its pressure chamber are shown in Figures 2.1 and 2.2, respectively.

Figure 2.1 - The High Pressure Tribometer

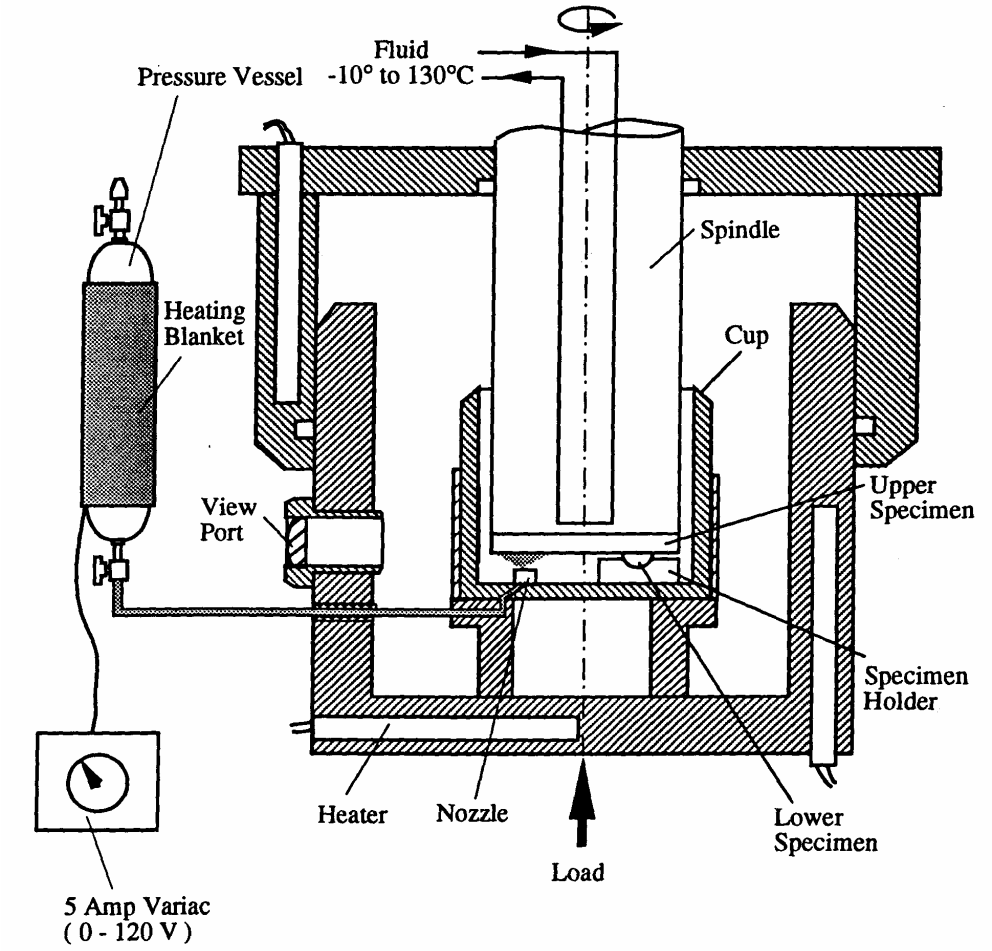

Figure 2.2 - Schematic of HPT Pressure Chamber and Lubricant Supply System

The HPT is capable of motion in two directions. The vertical or z-axis direction is used to access the samples, seal the high-pressure chamber, and provide the loading on the test specimens. The rotary or theta-axis direction controls the rotary motion of the upper sample. These displacements can be controlled manually via a control panel or through a computer. The lower stationary sample is mounted on a transducer module that measures the forces in the three orthogonal directions (F_x, F_y, F_z) and also the moment about the z-axis (M_z). The force F_z is in the normal or z-direction and the forces F_x, F_y are perpendicular to the z-axis. The resultant of F_x and F_y is called F_r, and is the friction force for generalized single point sliding. This positive value divided by the normal force F_z, provides the coefficient of friction (AMTI, 1991).

The test chamber is contained in a special pressure/vacuum housing capable of testing from 0.2 torr to 250 psi. Using a combination of heating and cooling systems, chamber temperatures from -12°C to 121°C can be attained. The desired temperature of the rotary contact specimen is obtained by pumping heat transfer fluid through the spindle. The temperature of the fluid is controlled by an external unit, which is capable of maintaining constant temperatures on the spindle from 30°C to 130°C. The chamber heaters consist of one 400-Watt cartridge heater in the upper chamber and two 400-watt cartridge heaters in the lower chamber. A lead screw that is driven by a DC servomotor through a harmonic drive supplies the normal contact load and unidirectional rotation. The specimen

mounting system has been designed to be general and consists of flat lower and upper surfaces with threaded holes to accept any specimens or fixtures for specimens. During an actual test, the lower sample is brought into contact with the upper sample using the motor driven lead screw located at the bottom of the unit. The maximum recommended load for this machine is 1000 lb_f, in addition to the maximum chamber pressure of 250 psi, which corresponds to a 7000 lb force that is needed to keep the chamber closed. The maximum unidirectional rotation is 2000 rpm. The HPT is equipped with computer control of the axial load and the angular velocity of the spindle. The computer control is achieved through control boards and a set of solid-state relays. The data acquisition card the computer uses is manufactured by National Instruments and its model number is AT-MIO-16F-5. This card has been discontinued since 1995. It was used since 1991 but was replaced in 2003 with a demo DAQ board that we obtained from National Instruments. The corresponding software allows for complicated loading and sliding velocity histories.

Figure 2.3 schematically depicts the four main subsystems that make up the tribometer. The first is the mechanical portion, which was described earlier and that contains the pressure chamber, sample holders, load sensors, position locators, temperature cartridge heaters for the upper and lower pressure chamber and the two drive motors that provide the vertical and rotary motion. The second section is the power box. This system contains the power amplifiers, power distribution system, fuses and relays. The chiller is used to maintain non-test portions of the tribometer at 20°C, which is achieved by re-circulation of heat transfer fluid in a closed loop. The last section is the control box, which contains the motor controls, amplifiers for load measurements, temperature controls and the microprocessor.

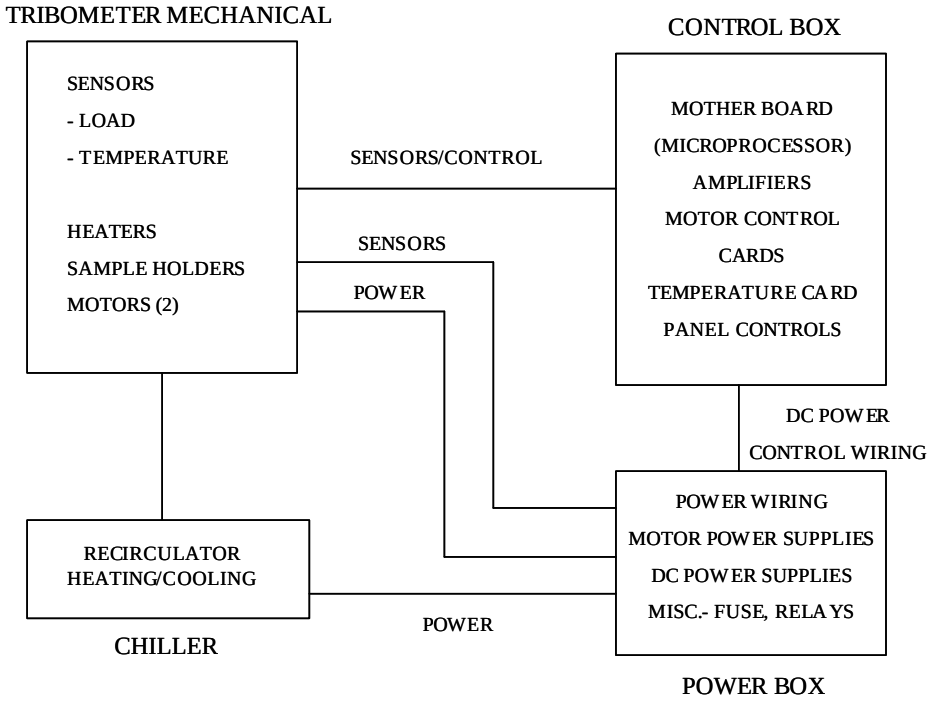

Figure 2.3 - The Four Main Sub-systems of the Tribometer

2.2 Contact Geometry

In this study, we use the pin-on-disc and the shoe-on-disk contact for the experimentation as shown in Figure 2.4. In this type of geometry thermal expansion of the specimen and other parts of the test rig do not increase any loading on the specimen (Yoon, 1999). In addition, the apparent area of contact does not change with time due to wear. Another advantage of this system is the fact that the rotating disc is the upper specimen, most of the wear debris falls at the base of the pins and the effect of debris accumulation from the experiment is eliminated.

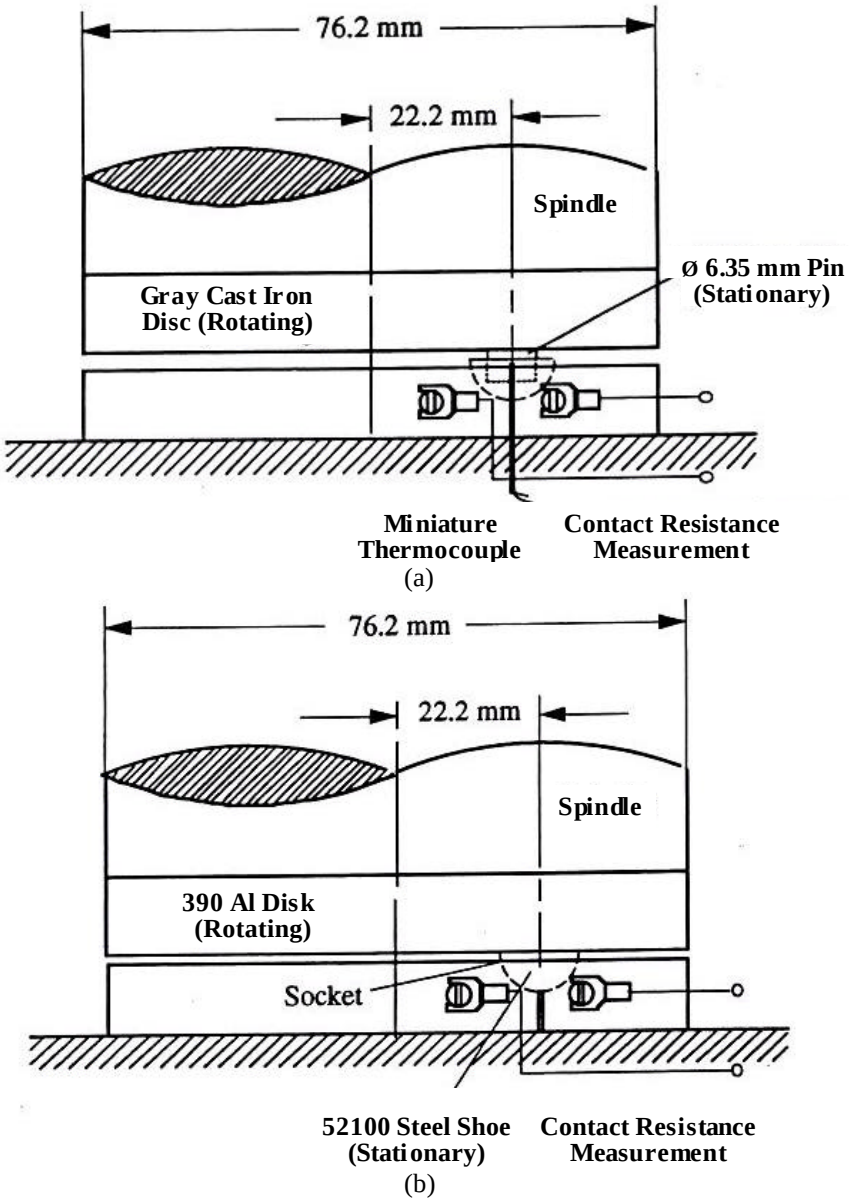

Figure 2.4 - Geometries of Contact (a) Pin-on-Disc, (b) Shoe-on-Disk

A photograph of the setup of the pin (or shoe) holder is shown in Figure 2.5. The base fixture consists of three pieces: the main base, an outer ring, and an O-ring (Buta-N) that serves as a seal in order to accommodate tests submerged in lubricant. When the pin-on-disk geometry is used, a miniature thermocouple can be inserted below the sliding surfaces to provide subsurface temperature measurements during testing as shown in Figure 2.4 (b). The

pins are inserted into a hole in the shoe, which, in turn, is supported in a socket as shown in Figure 2.5. An important point in this holder that should be noted is that the pin holder is self-aligning so that motion during contact is not restricted.

The specimen holder is electrically isolated by using a non-conductive material (Formica®) so that electrical contact resistance measurements can be provided, as it will be described below. Finally, depending on the type of test we can have a spraying nozzle or just a plug attached to the fixture. A small hole underneath the base fixture allows refrigerant or a mixture of refrigerant/lubricant to flow through and be sprayed near the contact area.

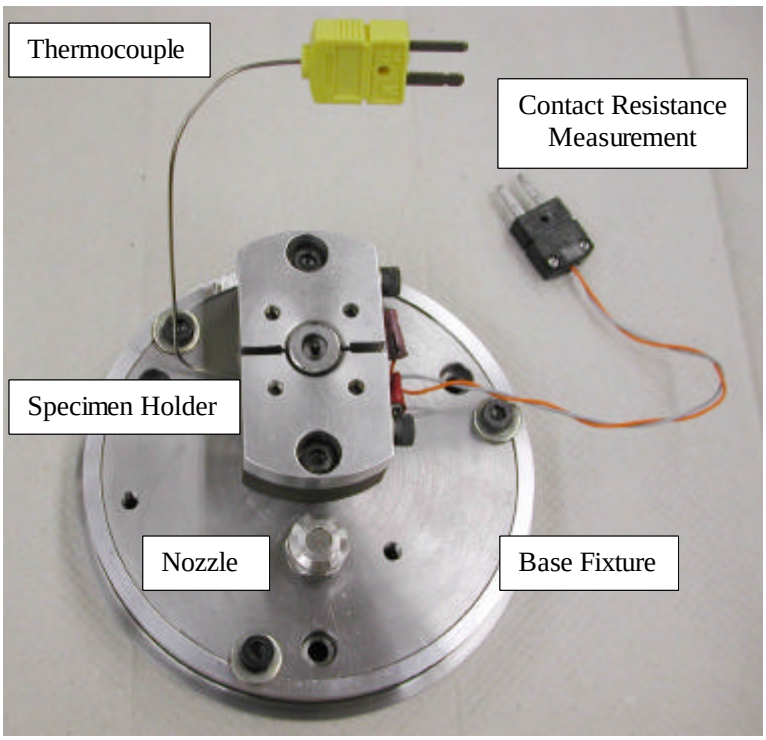

Figure 2.5 - Setup for Spraying Nozzle and Specimen Holder

2.3 Instrumentation

The instrumentation of the HPT includes a real-time output for the axial and friction forces, frictional torque, and the environmental temperature. The HPT is used to conduct scuffing experiments or simply run wear tests. In general, there are two ways that scuffing tests can be conducted in the HPT. One way is an endurance test, from which the time to failure is obtained for given constant load and velocity conditions. The other way is a step-loading test, for which the load is progressively increased stepwise for a specified sliding velocity until failure occurs. Figure 2.6 shows a typical endurance test, while Figure 2.7 shows a typical step-loading test. An endurance test corresponding to short time durations so that scuffing is avoided serves as a wear test for which the coefficient of friction can be obtained and wear can then be quantified by means of profilometry.

Scuffing can have various manifestations. The first obvious signs of scuffing are the increased audible noise and vibration. In a controlled laboratory environment, scuffing can be detected by sharp transitions in friction, contact resistance and near-contact temperature.

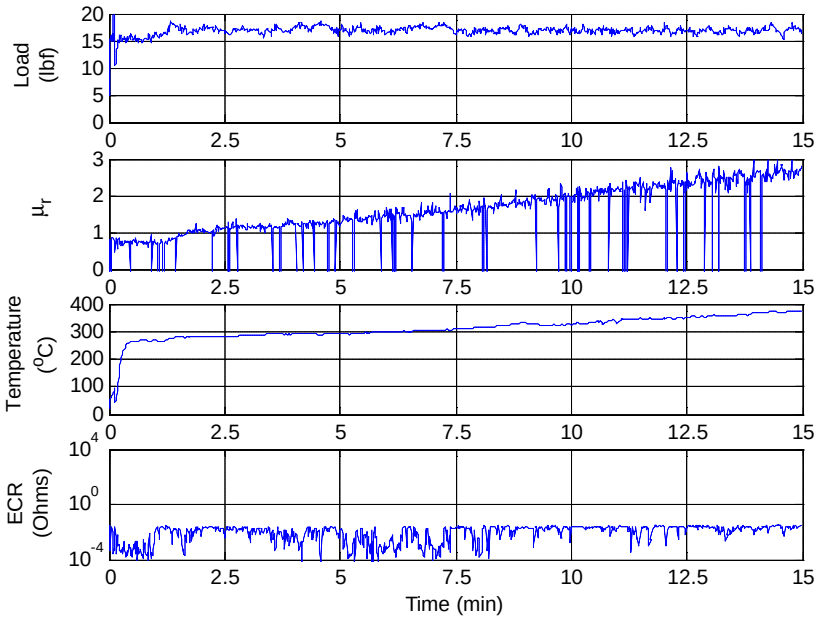

Figure 2.6 - Typical Endurance Experiment

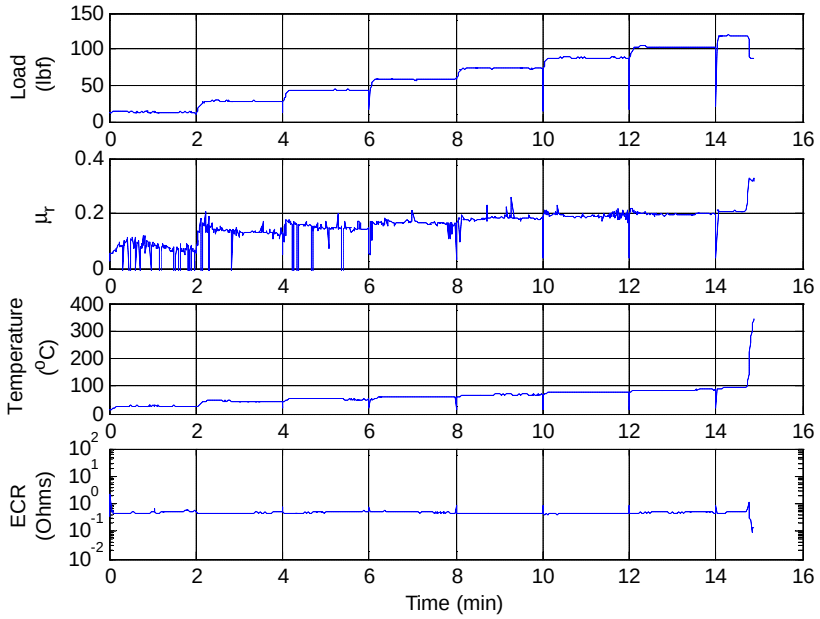

Figure 2.7 - Typical Scuffing Experiment

The electrical contact resistance (ECR) between the test specimens provides indirect information about the regime of lubrication, the formation of protective surface films and the extent of metal-to-metal contact. A schematic of the ECR measuring circuit is given in Figure 2.8. The measurement range of the circuit used is 10^{-6} – 10^{+4} Ω. This sensitivity was achieved by the development of a special four-terminal measurement circuit, methods for noise suppression and data processing software (Sheiretov, 1997). A large drop in the ECR is an indicator for scuffing. So the ECR is an important tribological quantity.

The surface temperature is also a very important tribological quantity. Its direct measurement in sliding interfaces is somewhat difficult. Due to experimental difficulties, the temperature in the vicinity of the sliding interface is often estimated with the aid of thermal models and subsurface temperature measurements. In practical situations, thermocouples are often employed to measure temperature.

2.3.1 Load vs. Time

As we mentioned the load can be applied two ways, either as constant or as step. Figure 2.6 shows a constant load of 17 lb_f while Figure 2.7 shows an increase in load every 2 minutes until scuffing.

2.3.2 Friction Coefficient vs. Time

The friction coefficient is a representation of the physical resistance to motion experienced by the pin in contact with the disk. Initially, for approximately 2 minutes, in the step loading case of Figure 2.7 the friction coefficient is erratic due to higher asperities. As these peaks are smoothened out the friction coefficient takes an almost constant value. This process is also referred to as run-in time (Cavatorta, 1997). In the case of a scuffed experiment like the one shown in Figure 2.7, the friction coefficient increases as the load increases until a maximum value is reached most likely depending on the shear strength of the material at which point the material cannot be loaded any further and the additional loading leads to scuffing. The friction coefficient can also increase with a constant load like the endurance test shown in Figure 2.6. Such behavior is tribologically possible when two identical materials are used. Once the oxides are removed, there is metal-to-metal contact and the coefficient of friction increases tremendously.

2.3.3 Temperature vs. Time

The temperature measured very close to the interface is also a good indicator of the contact severity. As we can see from both the endurance test and the step-loading experiment in Figures 2.6 and 2.7, respectively, the temperature increases as time progresses or as the load increases. During the experiment the temperature is somewhat stable and has a slow rate of increase. However, when scuffing occurs the temperature increases dramatically.

2.3.4 Electrical Contact Resistance (ECR) vs. Time

The ECR indicates the type of contact at the interface. More specifically, if the samples are fully separated by air or lubricant, the ECR is infinite. On the other hand, if the asperities experience significant contact the ECR should be zero. If the ECR is in the range of 10^{-2} to 10^{2} Ohms, two lubrication regimes exist. These are mixed and boundary. An ECR of 10^{-2} Ohms means a lot of asperities are contacting while 10^{2} Ohms means fewer asperities are contacting. These numbers are empirical and only relevant to our system. In Figures 2.6 and 2.7, the contact resistance is constant throughout the duration of the experiment. This means that there are several asperities in contact. As the asperities are worn the ECR remains constant. As subsurface failure occurs, the protecting layers are destroyed, leading to scuffing (Yoon, 1999). For the endurance test the value of the ECR is very low indicating severe contact during the entire test. That is because there was no lubricant film between the contacting surfaces. On the other hand, for the step-loading test, there was an initial lubricant film that was destroyed due to wear, and the surface smoothened out leading to a drop in the ECR at the point of scuffing.

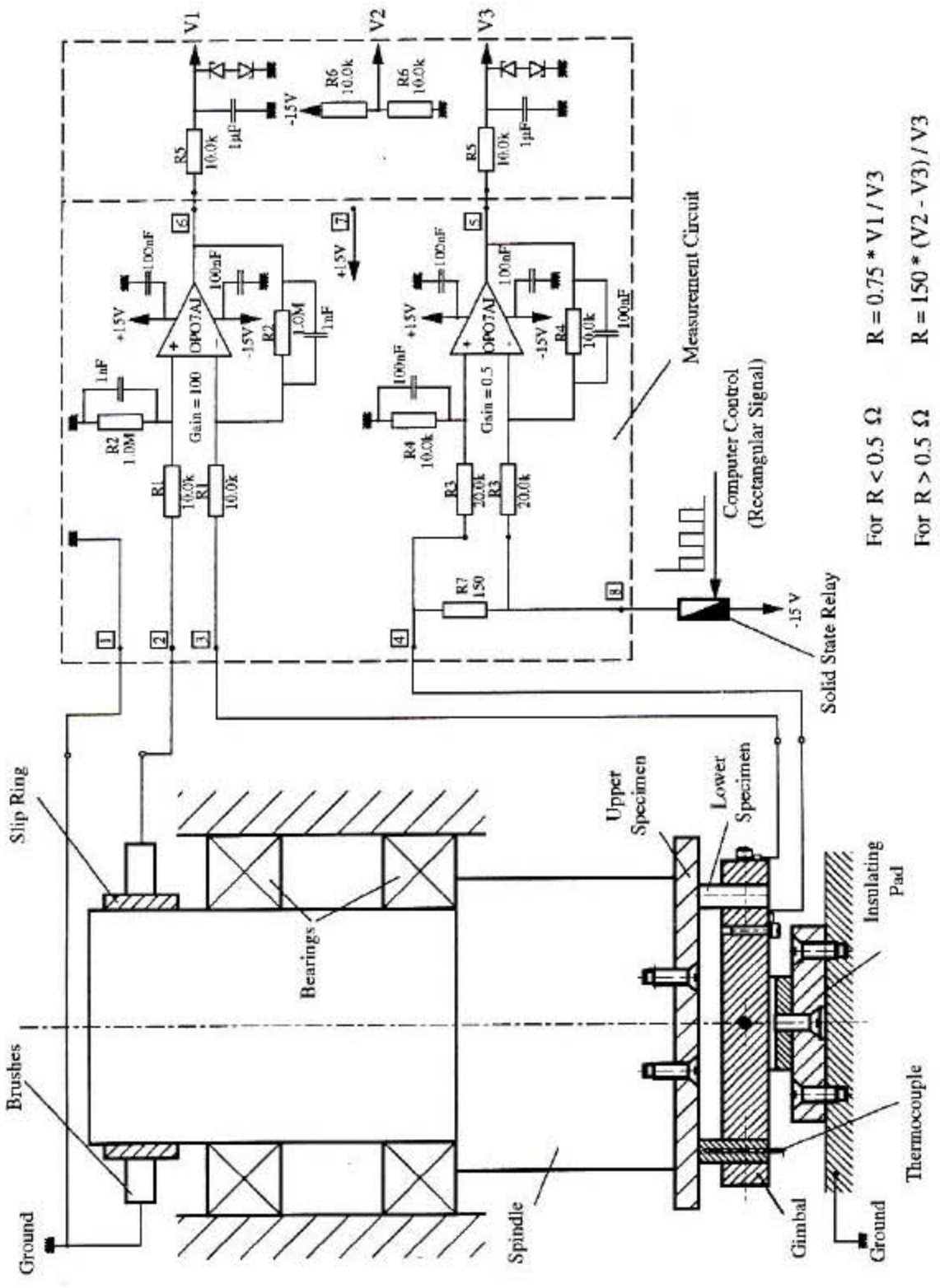

Figure 2.8 - Schematic of Electrical Contact Resistance Measuring Circuit

2.4 Experimental Procedure and Conditions

The pin-on-disc or the shoe-on-disk geometry was used to carry out the experiments in the HPT. For the pin-on-disk geometry both samples used were made of gray cast iron. For the shoe on disk geometry the shoes were made out of 52100 Steel and the disks were Al 390-T6. Typical samples of a disk, pin and shoe are shown in Figures 2.9 (a) and (b). The samples were prepared with the same machining process and had approximately the same roughness. The roughness for both the cast iron pins and disks was between 300-500 nm. The roughness of the Al disks was about 700 nm while the steel shoes were considered infinitely smooth. Some of the early experiments were performed using pins that were polished. Even though we tried to be consistent in the polishing, sometimes we noticed variation in the roughness. This may have influenced some of the early results, however, we tried to repeat the tests several times to ensure repeatability and we have included results that we think are representative.

All types of tests could be summarized into five categories depending on the experimental conditions. These five types are described in later sections.

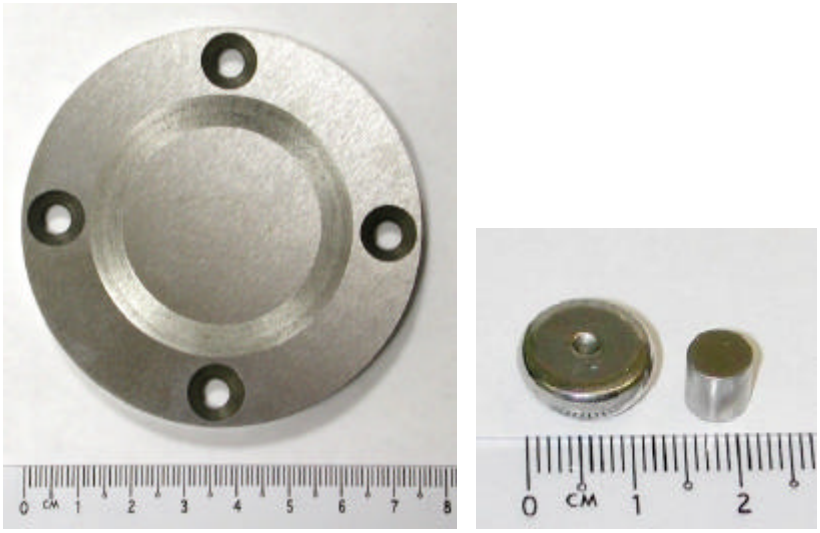

(a) (b)

Figure 2.9 – Typical Samples (a) Disk, (b) Pin and Shoe

Before initiating a test, the samples are pre-screened, optically and by contact profilometry, to ensure they have minimal surface damage from scratches. Then, the samples are immersed in pools of acetone and ultrasonically cleaned. They are rinsed with alcohol and dried using warm air. The samples are then placed in sealed containers to prevent contamination.

The running conditions for the samples in the HPT may vary. Different rotation speed, initial load, step load, environmental temperature and pressure have been used depending on the type of test. The different test conditions are described under the sections that correspond to the different types of tests. After the tribological testing the samples are again ultrasonically cleaned and used for wear quantification and surface topography measurements

2.5 Experimental Setups

Under this section five different types of tests are described in detail. These are: Type I-dry, non-lubricated under the presence of refrigerant, Type II-lubricated using spray of refrigerant only, Type III-lubricated using spray of refrigerant and lubricant, Type IV-fully submerged in PAG lubricant, and Type V-direct application of PAG lubricant via an absorbing medium.

The preliminary work of Cusano and Stokes (Cusano 1999) included Type III experiments. This type of test was developed by Cusano and has been used to accurately simulate the typical compressor conditions and test the performance of several material interfaces under the presence of refrigerants such as R134a and R410a. However, due to the difference in the thermodynamic properties, the Type III cannot be used with CO_2 as a refrigerant. That led to Type I and later on Type IV and V to avoid the complications that make the method of Type III inapplicable.

2.5.1 Preliminary Type I, II and III Experiments

There are two sets of preliminary tests. The first set was performed by Cusano and Stokes and the second set was performed by Poziemski and Reifman. Since the latter preliminary results consist of all types of test, they are described in detail in Sections 2.5.2 through 2.5.4 below.

In the experiments by Cusano and Stokes the weight of the CO_2/PAG mixture was between 405gr and 420gr, approximately 0.05% of which was oil. This corresponds to 40 mg/min and it was determined by trial and error since higher supply rates would result in no scuffing. Numerous experiments were performed and the test conditions for Type III of test are as follows:

- Initial normal load and step loading: 10 lb_f with 10 lb_f/15 sec
- Rotation speeds: 1.86 m/s, 2.79 m/s, 3.72 m/s and 4.65 m/s
- Chamber temperature: 120°C
- Chamber pressures: 25 psi

The step duration of 15 seconds is adequate because a steady state temperature is reached after approximately 10 seconds under starved lubrication conditions. When the CO_2/PAG mixture was used the tests were occasionally stopped before scuffing due to the depletion of the mixture in the pressure vessel. The pressure of 25 psi was used with the assumption that when the two refrigerants are compared, the pressure will not affect the results. Most tests focused in the use of CO_2 since R134a has continuously been used in the past and a great deal of experience has been obtained.

In the second set of preliminary tests that were performed by Poziemski and Reifman, a comparison between three different types of tests was investigated. This comparative study included Type I, II and III in CO_2 environment. Numerous experiments were performed and the test conditions for all types of test are as follows:

- Initial normal load and step loading: 10 lb_f with 10 lb_f/15 sec
- Rotation speeds: 2.4 m/s and 4.65 m/s
- Chamber temperature: 75°C
- Chamber pressures: 50 psi and 200 psi

2.5.2 Type I – Dry, Non-Lubricated under Presence of Refrigerant

The dry, non-lubricated tests are the simplest from all other types of tests and the preparation process requires very little time. For this type of test cast iron pins on cast iron disk samples were used. These basic experiments simulate the worse case scenario in a compressor.

1. The samples are prepared as described above in Section 2.4.
2. A plug is inserted to the base fixture to prevent leaks and also to ensure that a good vacuum is created once the chamber is closed. That is shown on Figure 2.10.
3. The prepared disk is placed onto the tribometer spindle and the sample pin is placed on the specimen holder. Then the base fixture is carefully placed inside the chamber. One should ensure that it sits properly and that the ECR cables will not be in the way of the spindle once the chamber closes.

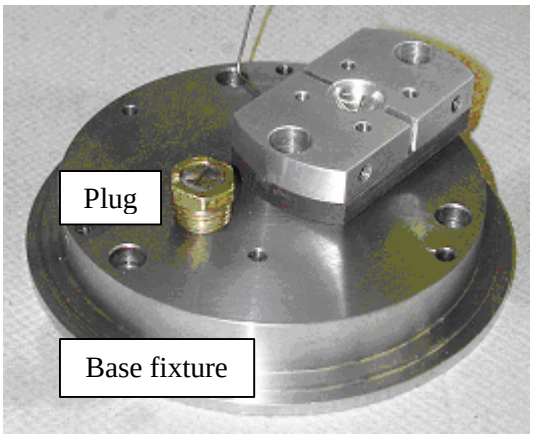

Figure 2.10 - Base Fixture

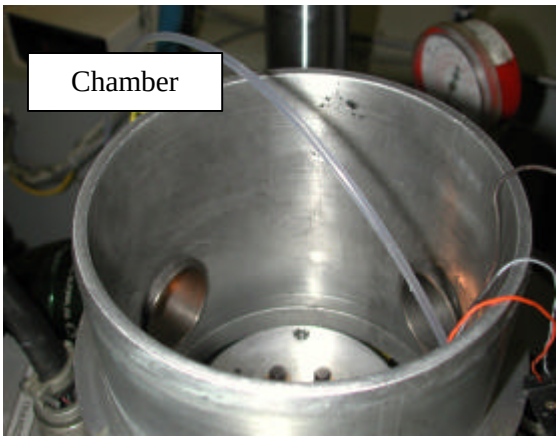

Figure 2.11 - Tribometer Chamber

4. Once the fixture is secured in place and tightened using the screws, the chamber is raised until it is properly closed.
5. The refrigerant is connected to the external HPT port.
6. A vacuum is created using a pump that is connected to the tribometer
7. The chamber is then filled with refrigerant to the required pressure.
8. Then the pin is brought in contact with the disk with an initial load of 10 lb_f.
9. Through the computer, the test is initiated.

The test conditions for this type of test are as follows:

- Initial normal load and step loading: 15 lb_f with no step
- Rotation speed: 1030 RPM (2.4 m/s)
- Temperature: 0°C, 60°C, 120°C
- Chamber pressures: 50 psi and 200 psi

These conditions are selected is via numerous trials under a chosen environmental condition. It was decided that a load of about 17 lb_f is reasonable since the material and the given geometry don't allow for a higher load. Any load higher than 20 lb_f would lead to immediate failure. Three different temperatures and two different pressures were selected for comparison.

2.5.3 Type II- Lubricated Using Spray of Refrigerant

This type of test is more complicated and much more time consuming than Type I. Type II should provide similar tribological performance as Type I and possibly better since the contact has a continuous flow of refrigerant. The weight and pressures below refer to the case of CO_2 and for other refrigerants would be significantly lower. However, the methodology is the same no matter what refrigerant one uses.

The following steps are necessary before every test using spray of refrigerant only:

1. A pressure vessel is rinsed with a few drops of 2-propanol and the contents are driven out with compressed air. When empty it should approximately weigh 6500 gr.
2. The empty vessel is then immersed in an ice bath.
3. The vessel is connected to a greater cylinder containing the refrigerant and the fill-up process begins.
4. After fill-up, the weight of the pressure vessel should be around 8250 gr. That means the weight of the refrigerant is 1750 gr. The pressure after fill up is around 800 psi.
5. The vessel is mounted on the HPT and connected to the inlet.
6. A heating blanket is attached to the vessel and the contents are heated at a voltage of 40% to 1520 psi as seen in Figure 2.12 below.
7. It is recommended that no more than a voltage of 50% be used to reduce the risk of burning the fuse. To achieve 1520 psi the heating process takes approximately forty minutes at 40%. The temperature of the contents at this pressure is approximately 70°C. At this point CO_2 is entirely in its gaseous phase as seen in the phase diagram presented earlier in Figure 1.1.
8. A nozzle is inserted to the base fixture to spray the refrigerant during the test.
9. Follow steps 3 through 6 of Section 2.5.2.
10. The spindle is set to rotate and the refrigerant is sprayed to lubricate the surface. This is done simultaneously ensuring that the pressure chamber gauge is kept under control so that the required pressure is not exceeded.

Figure 2.12 - Heating of the Pressure Vessel

11. Then the pin is brought in contact with the disk with an initial load of 10 lb_f.
12. Through the computer, the test is initiated.

The test conditions for this type of test are as follows:

- Initial normal load and step loading: 15 lb_f with no step
- Rotation speed: 1030 RPM (2.4 m/s)
- Temperature: Typically 75°C
- Chamber pressures: 50 psi and 200 psi

For this series of tests the shoe-on-disk geometry was used. Only a very limited amount of such tests was performed to examine how they compare to the Type I- dry, non-lubricated test. However, this type is also very aggressive and any load higher than 20 lb_f would lead to immediate failure of the material for the shoe on disk geometry.

2.5.4 Type III-Lubricated Using Spray of Lubricant and Refrigerant

This type of test is very similar to a Type II-Lubricated using spray of refrigerant only, with the exception that a small amount of lubricant is added into the pressure vessel before the refrigerant. The motivation for this type of test is that it simulates typical compressor conditions where a small amount of lubricant reaches the surface. After step 1 in Section 2.5.3, 5 mg of lubricant is weighted and then added to the clean pressure vessel. The vessel is placed into an ice bath and steps 3-12 are followed. For this series of tests the shoe-on-disk geometry was used.

The test conditions for this type of test are as follows:

- Initial normal load and step loading: 10 lb_f with a step increase of 10 lb_f/15 seconds
- Rotation speed: 1030 RPM (2.4 m/s) and 2000RPM (4.65 m/s)
- Temperature: 75°C
- Chamber pressures: 50 psi and 200 psi

2.5.5 Type IV-Fully Submerged in PAG Lubricant

This test requires a lot of care due to several reasons that will be described below. It serves as an ideal compressor case.

1. A plug is inserted to the base fixture as done previously in Section 2.5.2.
2. Then a tight fit of the glass around the base fixture is needed to ensure that no lubricant will leak out once the glass is filled with lubricant.
3. The prepared sample disk is placed onto the tribometer spindle and the sample pin or shoe is placed on the fixture.
4. The fixture is secured in place and tightened using the screws along with o-rings around the screws to prevent leakage.
5. Using a funnel, the desired lubricant is carefully poured into the glass until the specimen holder is fully covered and the pin or shoe, depending on the experiment, is completely submerged.
6. Then the chamber is raised until it is properly closed.
7. Follow steps 5-8 of Section 2.5.2. Note that when the vacuum check is initiated the oil starts bubbling. Basically the air that was trapped inside the oil starts coming out. The vacuum check will be complete even though air bubbles will continue coming out of the oil.
8. Through the computer, the test is initiated.

The test conditions for this type of test are as follows:

- Initial normal load and step loading: 50 lb_f with a step increase of 100 lb_f/2.5 minutes
- Rotation speed: 1030 RPM (2.4 m/s)
- Temperature: 90°C
- Chamber pressures: 200 psi

These conditions were also selected via several test trials. Even though these conditions are very aggressive there is hardly any detectable wear on the disk. So, a lower load is not recommended. Different times were performed for this type of tests to see the progressive wear pattern (Patel, 2000). However, no scuffing was attained with such experiments.

2.5.6 CO_2/Lubricant Re-circulation Supply Setup

One of the main concerns with using the experimental setup for Type-III experiments is miscibility. Experiments performed with the typical refrigerants like R134a or R410a showed that there are no complications due to miscibility issues using PAG oil. During previously done experiments it was observed that PAG might not be miscible in CO_2 and therefore a different experimental setup was proposed. Initially, it was thought that minor modifications of the High Pressure Tribometer (HPT) established lubricant/refrigerant supply system would provide us with a satisfactory lubricant supply system for CO_2 as well. The original supply system, established by Cusano and co-workers, consists of a pressure vessel, where a small quantity of lubricant is added to the refrigerant that is in liquid state. Heating of the pressure vessel increases the pressure in the vessel and enables the lubricant/refrigerant mixture to spray near the contact interface. However, such a supply system does not guarantee miscibility of the CO_2/lubricant. Furthermore, during the spraying from a very high pressure of over 1500 psi inside the pressure vessel into the tribometer (which is at 50 psi or 200 psi) leads to a "blowdown" condition that does not guarantee fixed known thermodynamic conditions inside the tribochamber. Even though a "blowdown" condition takes place when other refrigerants like R134a or R410a were used, miscibility was not an issue. This has been extensively discussed in Chapter 3. The development of an alternative system where the lubricant is placed in the tribochamber (sump) along with the desired CO_2 pressure then is circulated using a micropump, as shown schematically in Figure 2.13 was found to be a rather tedious task and not at all as trivial as initially expected.

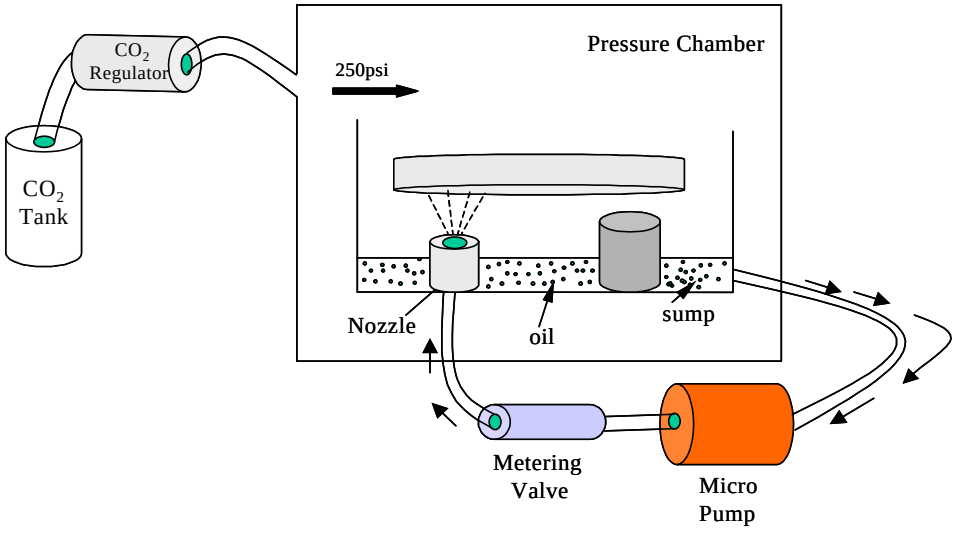

Figure 2.13 - Experimental Setup for CO_2/Lubricant Supply System

There were some difficulties in developing the new CO_2/lubricant supply system. Several problems with sealing were encountered and the design of a new fixture was necessary to correct the occurring leaks. The fixture was designed to be adjustable and allow the oil sump to remain inside the High Pressure Tribometer chamber

without leaking. Filter selection was another really important issue that had to be resolved. As the pin and disk make contact, there is debris that can be potentially harmful for the pump so a 10-micron stainless steel filter becomes necessary before the inlet of the gear pump. Two filters were used. Both of these filters were ordered from Upchurch Scientific. The first one was made out of PEEK. This filter can draw solvent to within 2 mm of the bottom of the solvent bottle. The maximum flow rate of the 10 mm filter is 100 ml/min. The part number for this filter is A-438. The second filter was made out of 316 stainless steel. This filter can draw solvent to within 3.2 mm of the bottom. The part number for this filter is A-550. In order to use, we simply press fit the Teflon tubing firmly into the top holes.

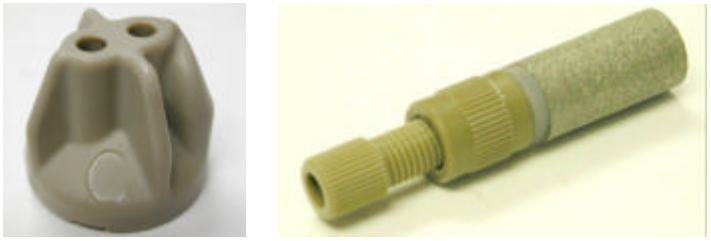

(a) (b)

Figure 2.14 - Filters Used in the Re-circulation Setup (a) PEEK (b) Stainless Steel

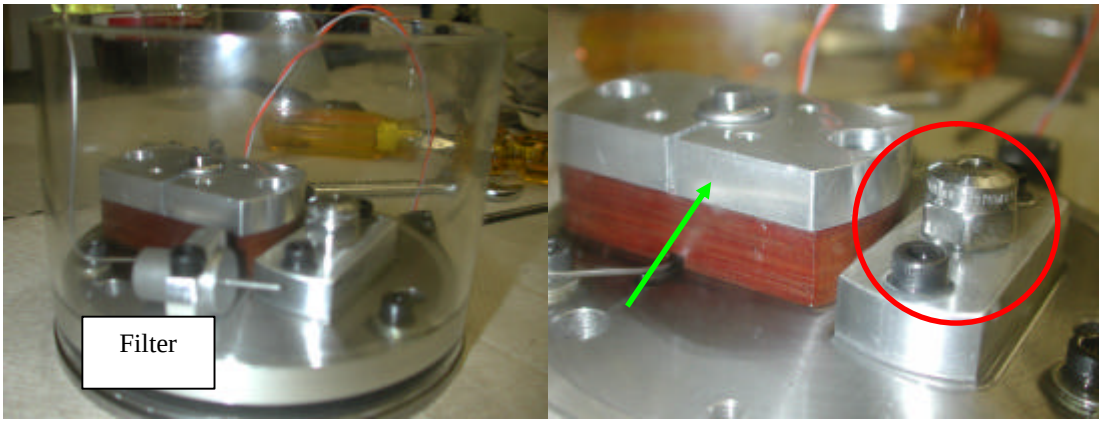

Figure 2.15 - Modified Fixture for New Lubricant/CO_2 Supply System

However, due to space limitations, as it can be seen in Figure 2.15, a longer pin holder had to be designed to allow full submersion of the filter while the pin is not submerged as pointed out with a green arrow in the same figure. In this figure we can also see a special adapter (red circle) for extending the nozzle above the level of the oil so that it is not submerged when the filter is fully submerged.

Furthermore, many different adapters, connectors and pipes had to be selected to create a setup that would be compatible with both the HPT and existing pumps. During this stage, two types of pumps were tested. These were a piston pump and a gear pump. The piston pump was quickly eliminated even though it provides very small flow rates because a continuous flow was needed. Experiments with the gear pump were attempted but the setup still needed some refinements. The orifice size of the nozzle was also another issue that could not be resolved. That creates a pressure built up in the outlet and along the lines of the pump that results in leakage through the pump.

This setup did not work because of the high pressure differential needed to pump the oil back into the chamber as an atomized spray, so no results have been obtained.

2.5.7 Type V-Direct Application of PAG Lubricant via Absorbing Medium

This type of experiment requires special care since there is no previous experience with the setup used. This is perhaps the "ideal" experiment. The need for boundary and mixed lubrication with CO_2 is fulfilled and stable thermodynamic conditions are achieved. The following steps are needed:

1. We cut an absorbing medium with approximate diameter of 2.5 inches. This is a commercially available type of woven cloth with a medium density.
2. The medium is inserted inside a holder and tightened on the base fixture as shown in Figure 2.16 below.
3. We ensure that the height of the cloth is slightly higher than the specimen holder so that it will make contact with the disk before the pin. However, it is important to ensure that the cloth does not exceed a certain height, as this will cause a lot of damage to the cloth once the disk starts rotating.
4. We measure approximately 50 mg of PAG lubricant in a beaker and with a syringe we apply the oil to the absorbing medium. This corresponds to 3 drops of lubricant using a regular syringe.
5. We follow steps 2 through 7 of Section 2.5.2.
6. Then we bring the absorbing medium in contact with the disk and allow the disk to rotate a couple of times to get a lubricant film on the disk.
7. Then we bring the pin into contact with the disk with an initial load of 20 lb_f.

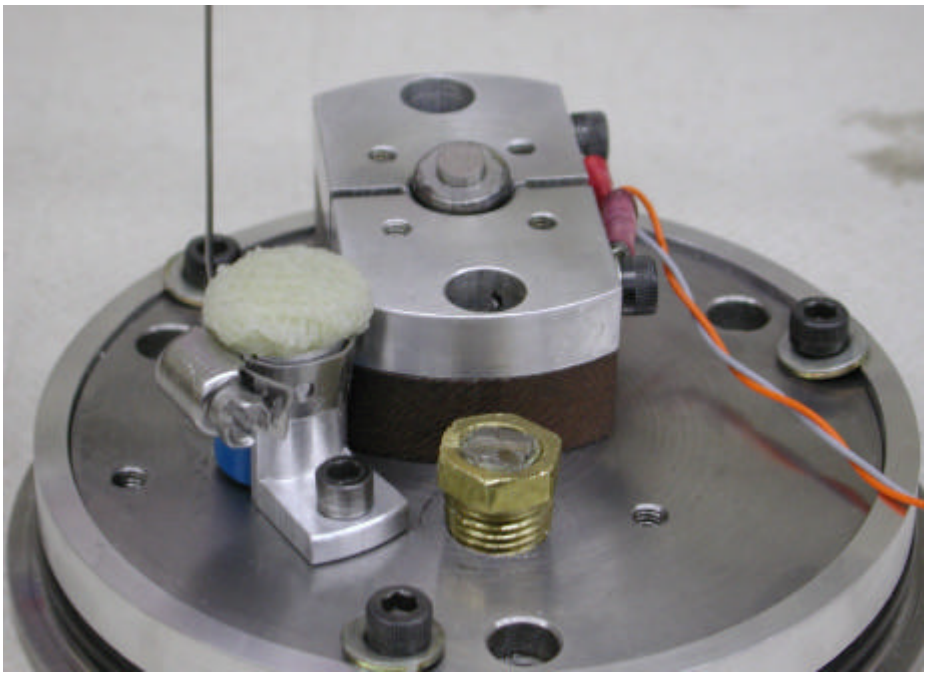

Figure 2.16 - Setup for Direct Application of Lubricant via Absorbing Medium

8. Through the computer, the test is initiated.

The test conditions for this type of test are as follows:

- Initial normal load and step loading: 20 lb_f with 35 lb_f/30 sec
- Rotation speed: 1030 RPM (2.4 m/s)
- Temperature: 120°C

- Refrigerant: R134a, CO_2
- Chamber pressures: 25 psi (R134a), 200 psi (CO_2)

Through trial and error it was realized that approximately 50 mg of oil is adequate to create a lubricant film. The ECR was a useful indicator to realize that 50 mg is the amount needed since it places the contact in the mixed boundary lubrication regime. If more oil is used, there is no detectable wear even with very high loads. The loading conditions were also selected via numerous trials. Aggressive conditions are needed and the chosen 35 lb_f/30 sec increase seems to be satisfactory for the amount of oil used for this test. R134a was selected for the comparison.

Chapter 3. Results and Discussion

3.1 Introduction

All of the 5 different types of tests were performed in order to better understand the behavior of CO_2 and how it compares with other refrigerants. Due to the thermodynamic complexities involved in Types II and III and the discrepancies observed in some preliminary work during the Type III test, we tried to isolate some of the thermodynamics, which initially led us to performing Type I and later on Type IV and V tests.

The Type III test was developed more than a decade ago by Cusano and has extensively been used in the past to test the performance of numerous material interfaces under the presence of refrigerants such as R134a and R410a. However, it was never used with CO_2 as a refrigerant. As previously mentioned in Chapter 1, CO_2 is thermodynamically much different than the refrigerants above, for which a great deal of knowledge has been gained by the continuous work with them. When involvement with CO_2 was engaged it was not anticipated that it would be much different and that the previously developed method for testing could be applied as well. Unfortunately, this was not true. The existing method could not be applied to CO_2 and the reason for that was immiscibility coupled with the fact that under the conditions used for spraying in a Type III test, CO_2 was in its gaseous state unlike the other refrigerant which were in liquid state. In the preliminary work, the importance of miscibility was not realized and numerous experiments were performed using the setup described in Section 2.5.4. These have been discussed below.

After the basic Type I tests, the issue of miscibility had to be examined. The initial thought was to deliver the oil in the surface separately while the chamber was in the presence of refrigerant. So a re-circulation setup was proposed that would have the lubricant in a sump and then through a pump we would provide it to the surface while the chamber was pressurized with refrigerant. After some effort it was realized that due to the high pressure differentials needed to pump the oil back into the chamber as an atomized spray this setup cannot work. That led to Type IV and V tests.

3.2 Preliminary Experiments-Main findings

3.2.1 Cusano-Stokes Experiments (1999)

The scuffing resistance of R134a was compared to CO_2 under the presence of PAG lubricant. Consistent data could not be acquired for the tests conducted using a CO_2/PAG mixture and a satisfactory explanation for the inconsistency could not be offered. It was proposed that this inconsistency is due to lack of understanding of CO_2 in the system. However, it was noted that in spite of the scatter within the data, the results indicated that the CO_2/PAG mixture has better lubricative properties than the R134a/PAG mixture. During this work it was observed that the friction during the progression of the tests utilizing the CO_2/PAG mixture was lower than the tests using the R134a/PAG mixture.

The curve for CO_2 could not be fitted due to the large scatter as well as the high number of tests that did not scuff before the CO_2/PAG mixture ran out. On the other hand, the scuffing data for R134a/PAG mixture maintained an approximate PV=constant relationship. As the sliding velocity increases, the scuffing pressure decreases. Despite the scatter, a similar trend was ascertained from the CO_2/PAG data. For the same velocity nearly all results

failed at pressures higher than the scuffing pressures using R134a. The results can be seen in Figure 3.1 where a pressure-velocity diagram is presented for the two mixtures.

As we previously mentioned, immiscibility is the most probable reason that makes this method for testing under the presence of CO_2 inappropriate. After the filling process, CO_2 exists inside the pressure vessel as liquid and gas. So, initially the liquid CO_2 is mixed with the lubricant but as the heating process takes place to raise the pressure so that it can be sprayed, the liquid CO_2 turns into gas and the lubricant remains on the bottom of the vessel.

A possible explanation to what follows is that when the valve is opened and the contents are sprayed, the lubricant comes out all at once first, and then CO_2 gas is continuously sprayed coming out of the nozzle as dry ice that instantly turns again into gas since the chamber temperature is high.

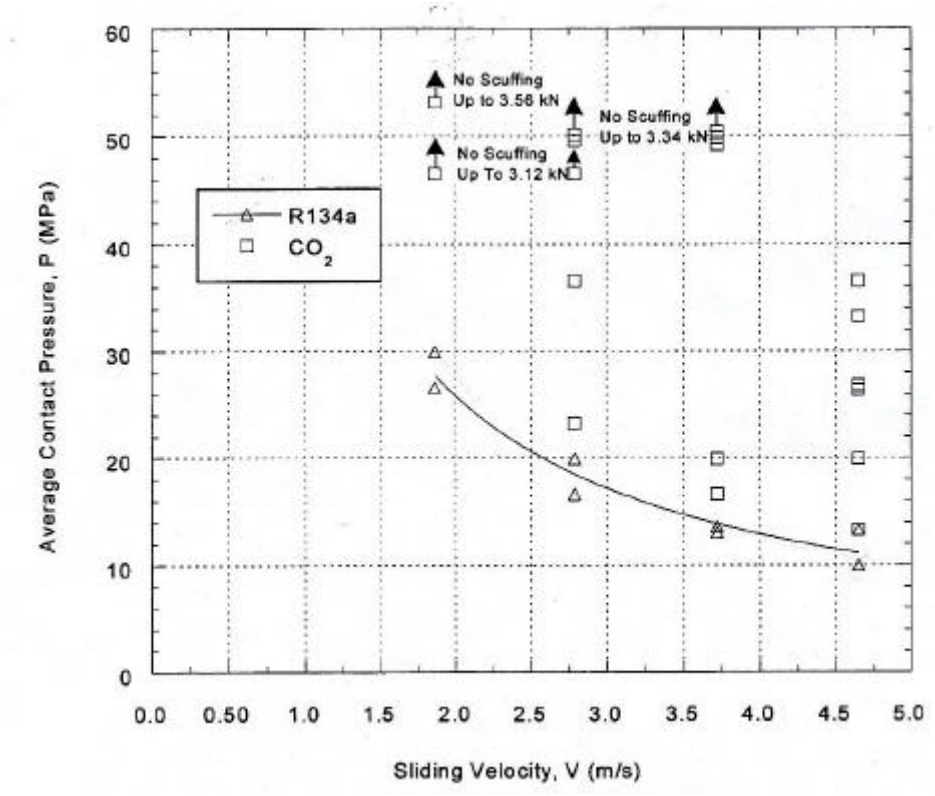

Figure 3.1 - Scuffing Pressure-Velocity Diagram for Al 390-T6 and 52100 Steel in R134a/PAG or CO_2/PAG

In the preliminary results by Cusano and Stokes it is almost evident that this is what takes place in the results obtained for CO_2 from the low coefficients of friction achieved. When the lubricant is initially sprayed onto the surface it takes quite some time until scuffing and since the lubricant/refrigerant spray is not uniform during the duration of the test like in the case of R134a but comes out all at once, the friction coefficient remains low.

3.2.2 Poziemski-Reifman Experiments (Summer 2001)

During the preliminary work by Poziemski and Reifman, Type I, II and III were performed to further investigate the previously observed scatter in the data by Cusano and Stokes. The methodology and the way this experiments were carried was once again the same as the method utilized by Cusano and Stokes. For Type II and III the refrigerant undergoes the same phase changes when heated and sprayed. From its initial two phase (liquid and

gas) it is heated at which point there is only gas and then sprayed becoming dry ice that quickly turns into gas due to the high chamber temperature. So, these series of tests resulted in scatter for Type III as we could have expected for the same reasons as previously explained in section 3.2.1. The thermodynamics are the same for the Type II tests as well.

All three types of experiments (I, II, and III) were performed at 2 different speeds (2.4 m/s and 4.65 m/s) and are depicted in a P-V diagram in Figure 3.2 below. Each point in the graph corresponds to a single experiment.

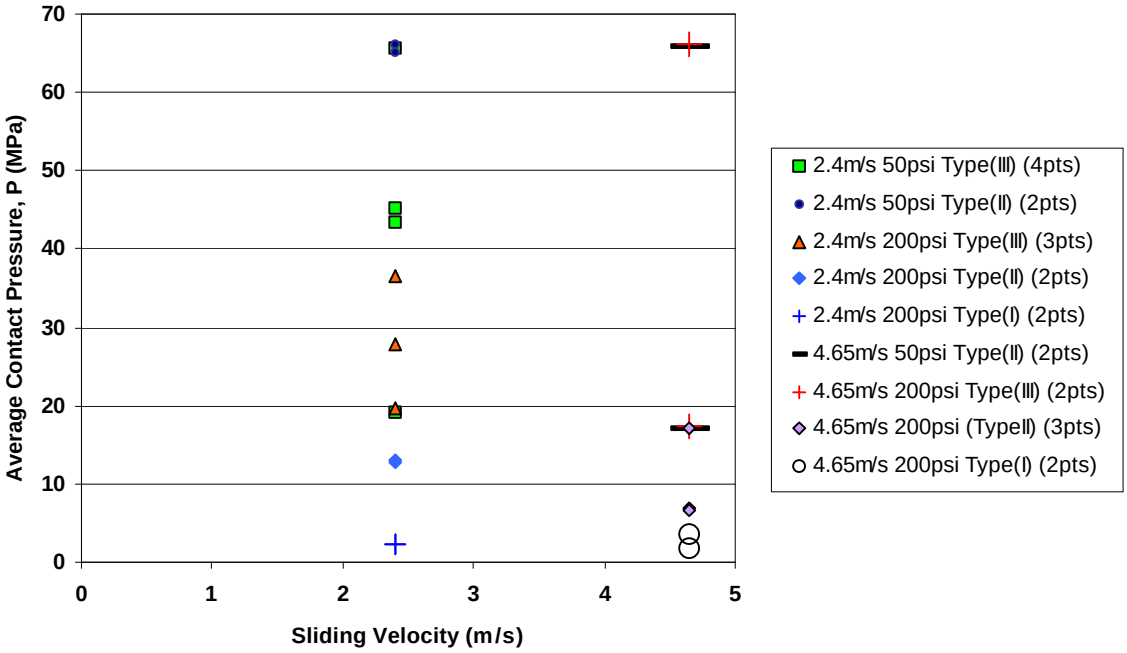

Figure 3.2 - Scuffing Pressure-Velocity Diagram for Al 390-T6 and 52100 Steel in CO_2/POE

The average contact pressure on the y-axis corresponds to the maximum normal load at which scuffing occurred divided by the nominal contact area. If we closely examine Figure 3.2, we can observe that consistent data occur only for Type I and II experiments. For 2.4 m/s, Type I (CO_2 presence alone) and Type II (CO_2 spray) experiments produce very repeatable data points, where scuffing occurred at the pressures of about 3 MPa, and 13 MPa, respectively. On the other hand, for Type III experiments (CO_2/POE spray) the results of three experiments are not very repeatable with scuffing varying between 20-37 MPa. When the same experiments were repeated at the higher speed of 4.65 m/s, the repeatability is once again seen for Type I and II experiments only. For Type III experiments, the two experiments that were performed produce very different results.

So, Type III experiments exhibit large scatter, similar to the scatter reported by Cusano and Stokes using CO_2/PAG oil. From the experiments above we note that the performance of Type III is better than Type II, which, in turn is better than Type I. The consistency of Type I experiments gave the motivation for the next experiments described in Section 3.3.

3.3 Type I-Dry, Non-Lubricated under Presence of Refrigerant

In order to avoid the aforementioned thermodynamic complexities, Type I experiments were conducted. This is a very basic type of experiments that was performed in order to better understand the behavior of CO_2 and also compare its lubricative properties with previously used refrigerants. The cast iron pin-on-disk geometry was used for these tests.

During this type of test, there is no phase change since the chamber pressure is constant at a known fixed value. There are no thermodynamics involved during this type of test and the conditions (temperature and pressure) are known at any give time. Nonetheless, a drawback with this type of test is that the absence of lubricant does not allow for high loads and only very low loads can be sustained by the material interfaces used in this work. This is the worse case scenario for compressors.

Numerous experiments of this type were performed. The early experiments were performed using pins that were polished and in many instances there was variation in the roughness. This may have influenced some of the early results, however, we tried to repeat the tests several times to ensure repeatability and we have included results that we think are representative. First we studied the effects of temperature and pressure and then we compared CO_2 with R134a and air.

3.3.1 Effects of Temperature and Pressure

Three different temperatures namely 0°C, 60°C and 120°C selected as low, medium and high respectively, while two different pressures, 50 psi and 200 psi, as low and high respectively were examined. For the case of 50 psi we can see the effect of temperature in our results. This can be seen in Figures 3.3 through 3.5 below. At 0°C, the coefficient of friction is low taking values between 0.1 and 0.25 while the near-contact temperature also remains low around 50°C. At 60°C, the coefficient of friction is higher than the 0°C case taking a value of about 0.5 while the near-contact contact temperature is significantly higher this time with a value of about 200°C. For the case of 120°C, the friction coefficient is the highest from the other two cases taking a value of about 1 while the contact temperature reaches 300°C.

So, for the case of the lower pressure of 50 psi the results seem to indicate that as temperature increases, the coefficient of friction and the near-contact temperature both increase. That is what one could have expected at this range of temperatures. For the case of 0°C it is possible that water due to condensation was acting as a lubricant creating a film between the interacting surfaces. Condensation was visible before initiation and during the experiment. However, for the case of 60°C and 120°C there was no condensation, and the results seem to follow the expected trend.

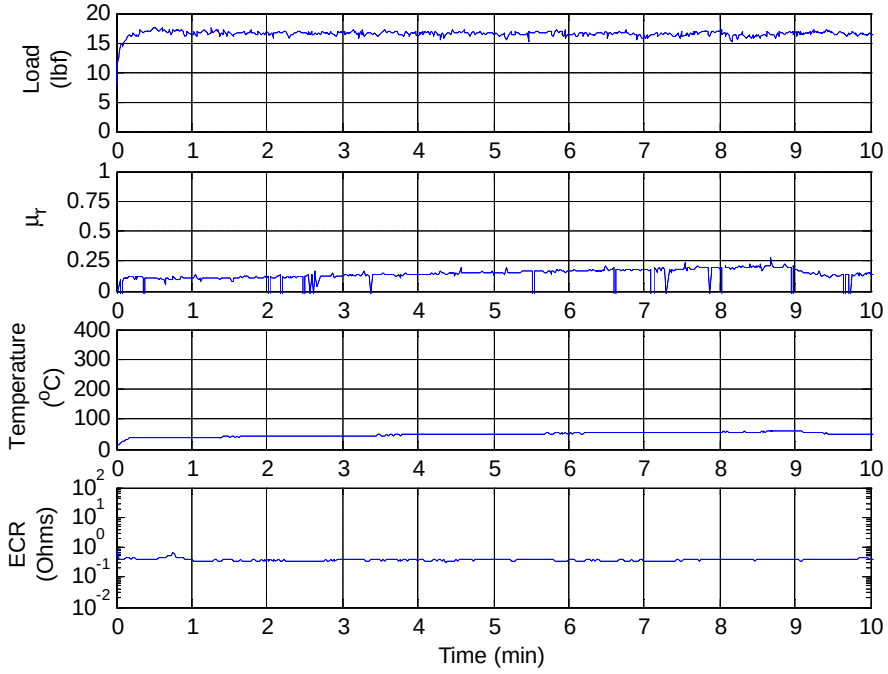

Figure 3.3 - CO_2, 50 psi, 0°C

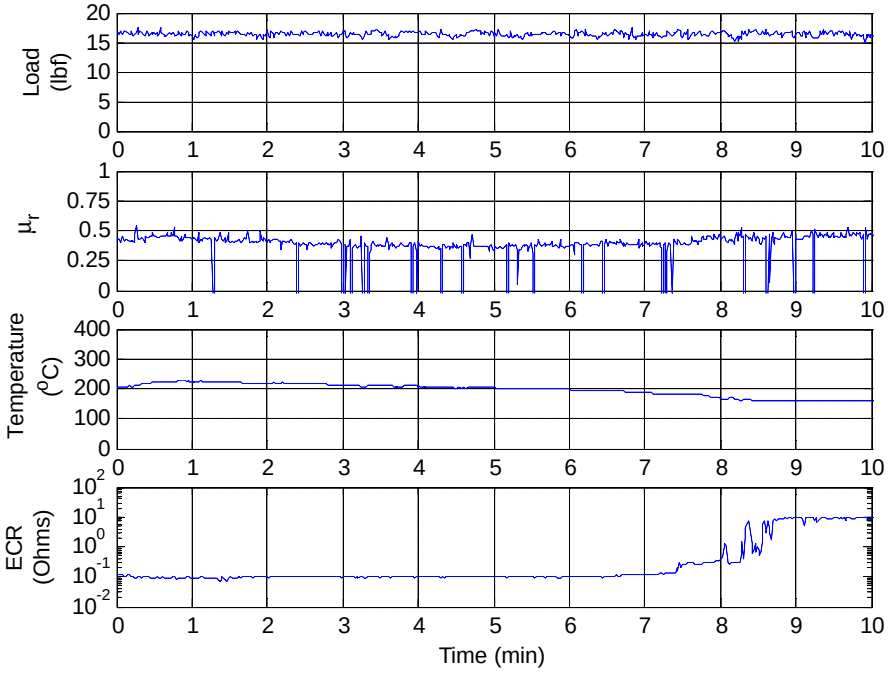

Figure 3.4 - CO_2, 50 psi, 60°C

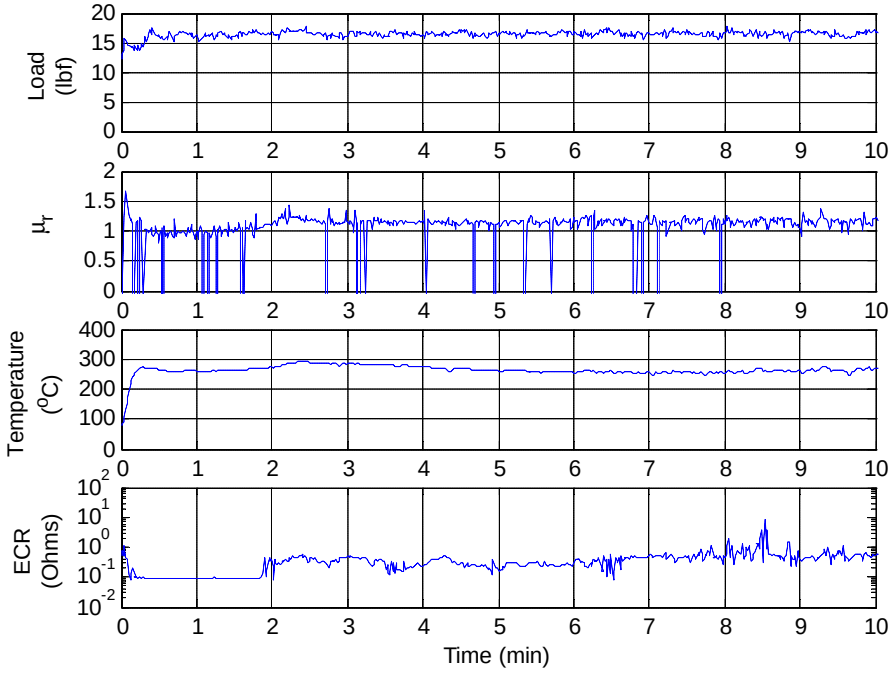

Figure 3.5 - CO_2, 50 psi, 120°C

For the selected pressure of 200 psi a similar trend is observed. This can be seen in Figures 3.6 through 3.8. At 0°C, the coefficient of friction is low taking a value of 0.1 while the near-contact temperature also remains low around 25°C. At 60°C, the coefficient of friction is higher than the 0°C case taking a value between 0.25 and 0.4 while the near-contact temperature is higher this time with a value of about 100°C. For the case of 120°C, the friction coefficient is the highest from the other two cases taking a value of about 1 while the near-contact temperature reaches 200°C.

So, for the case of the higher pressure of 200 psi it also becomes clear that as temperature increases, the coefficient of friction and the contact temperature both increase.

By examining Figures 3.3 through 3.8 we can also note that the higher pressure seems to have a slightly positive effect on the sub-surface temperature. We may note though that the coefficient of friction remains approximately the same for both pressure cases.

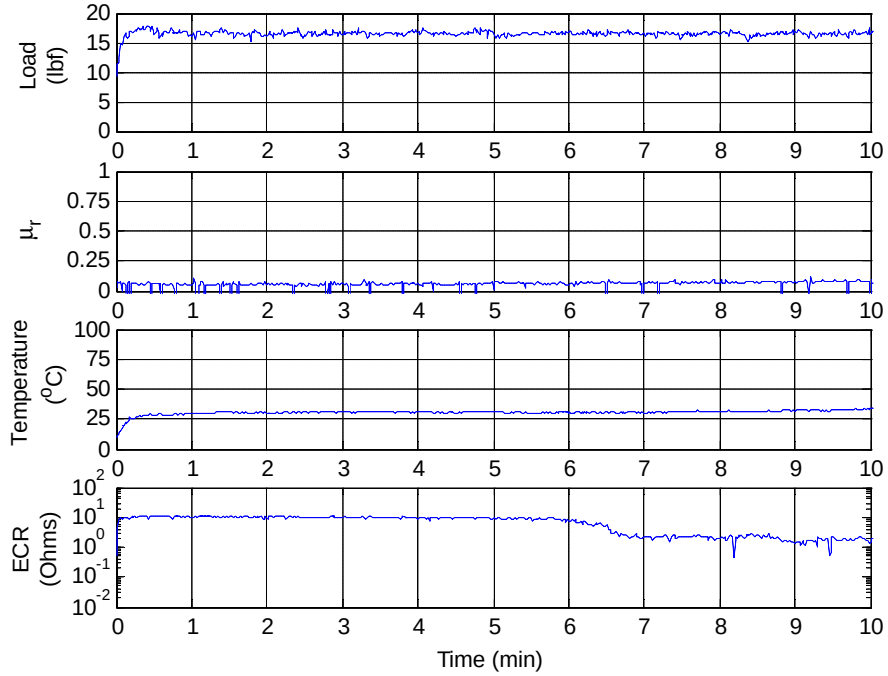

Figure 3.6 - CO_2, 200 psi, 0°C

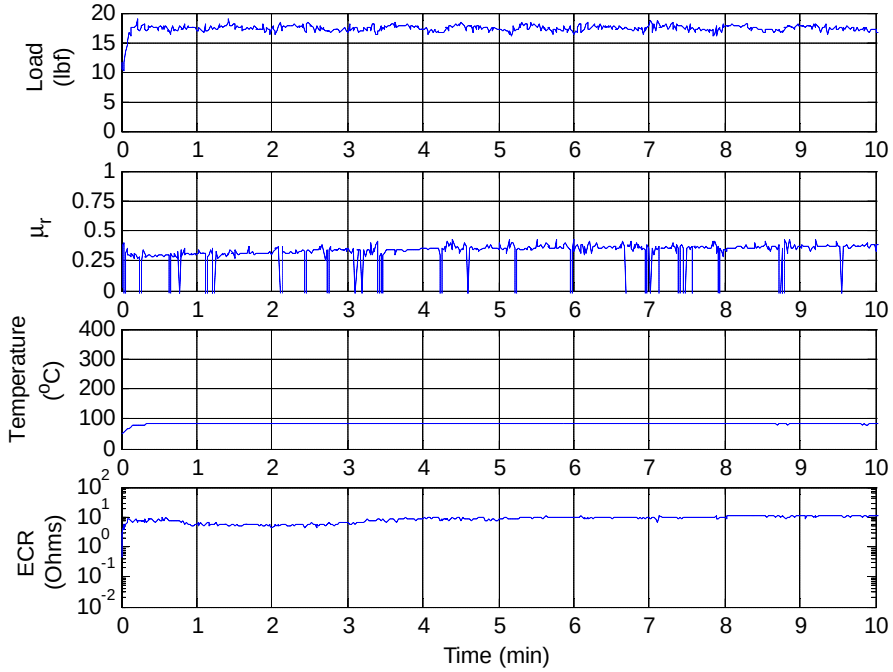

Figure 3.7 - CO_2, 200 psi, 60°C

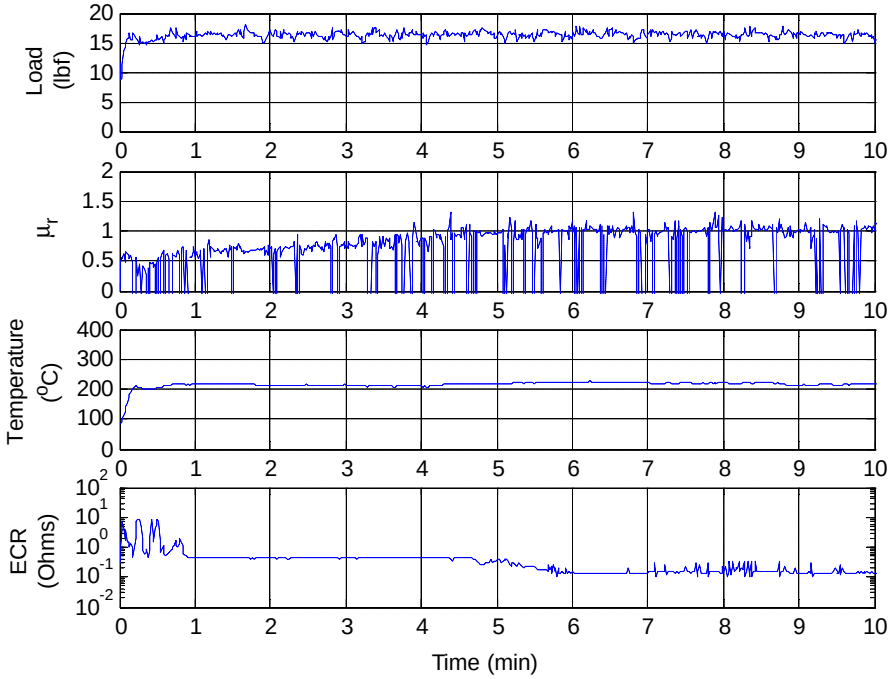

Figure 3.8 - CO_2, 200 psi, 120°C

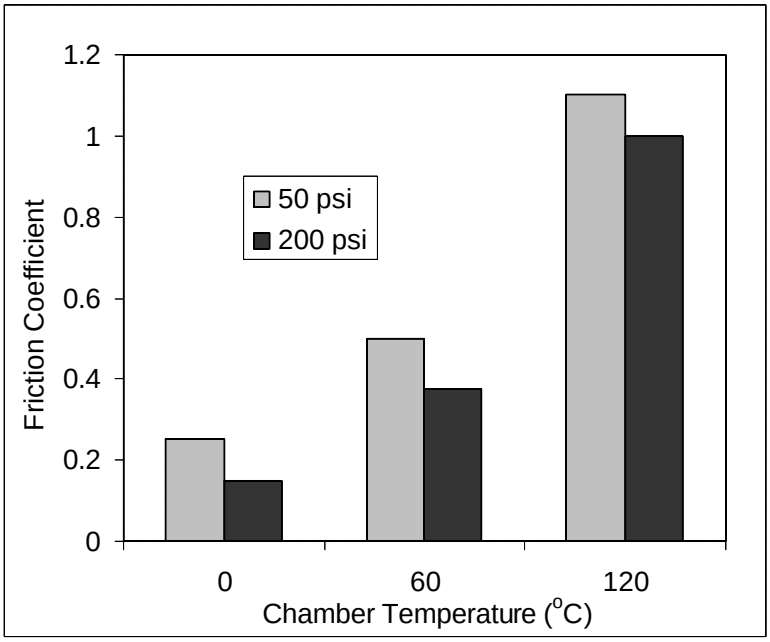

Figure 3.9 - Friction Coefficients for Constant Load Tests for CO_2 at Different Operating Conditions

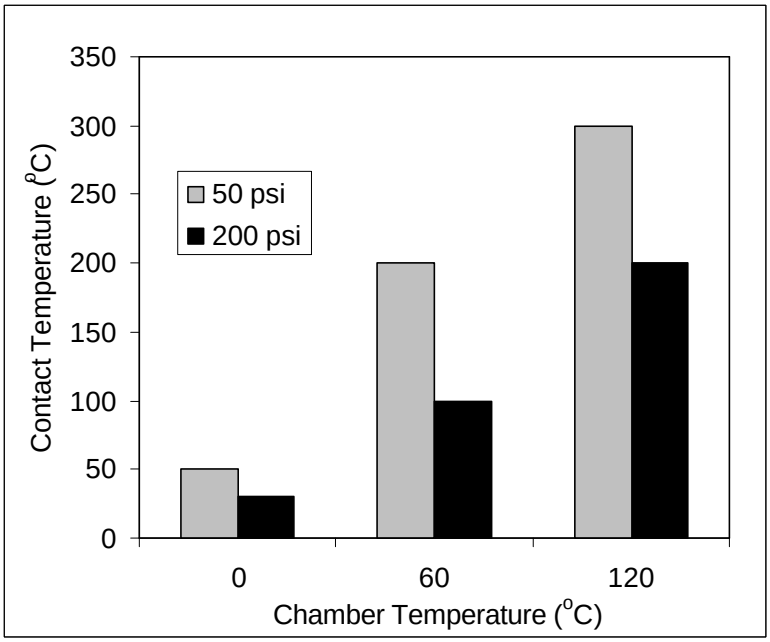

Figure 3.10 - Contact Temperatures for Constant Load Tests for CO_2 at Different Operating Conditions

Two experiments for each of the different conditions were performed. In general, the results were similar and we believe we have included representative tests. However, one should keep in mind that it is possible that some of these tests were performed using samples that were not identically prepared. Roughness variations are likely to have occurred due to polishing and some disks may not have had the coating mentioned above.

The results for the different pressures and temperatures have been summarized in Figures 3.9 and 3.10.

3.3.2 Comparison of CO_2 with R134a and air

The test protocol developed more than a decade ago by Cusano and co-workers that has extensively been used in the past to test the performance of numerous material interfaces under the presence of refrigerants such as R134a was never used with CO_2 as a refrigerant. As previously mentioned, CO_2 is thermodynamically much different than commonly used refrigerants. The existing method could not be applied to CO_2 and the reason for that was immiscibility of lubricant coupled with the fact that under the conditions used for spraying, CO_2 was in its gaseous state unlike the other refrigerants, which were in liquid state. In order to avoid the issue of immiscibility, controlled experiments at constant loads in the presence of CO_2, R134a and air were performed. CO_2 was compared with refrigerant R134a and air under Type-I, dry non-lubricated test. R134a was tested at 60°C and 25 psi the same way CO_2 was tested at 50 psi. Air was tested at ambient pressure and 60 °C. The results obtained for CO_2 are shown in Figure 3.11 while the results for R134a are shown in Figure 3.12. If we compare the two figures we will see that the two refrigerants performed quiet similarly.

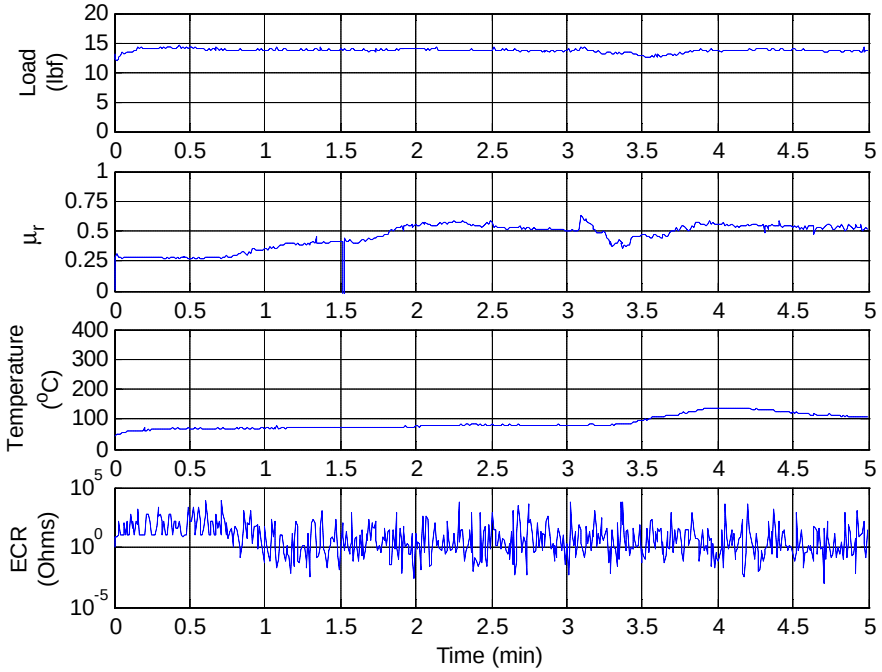

Figure 3.11 - CO_2, 50 psi, 60°C

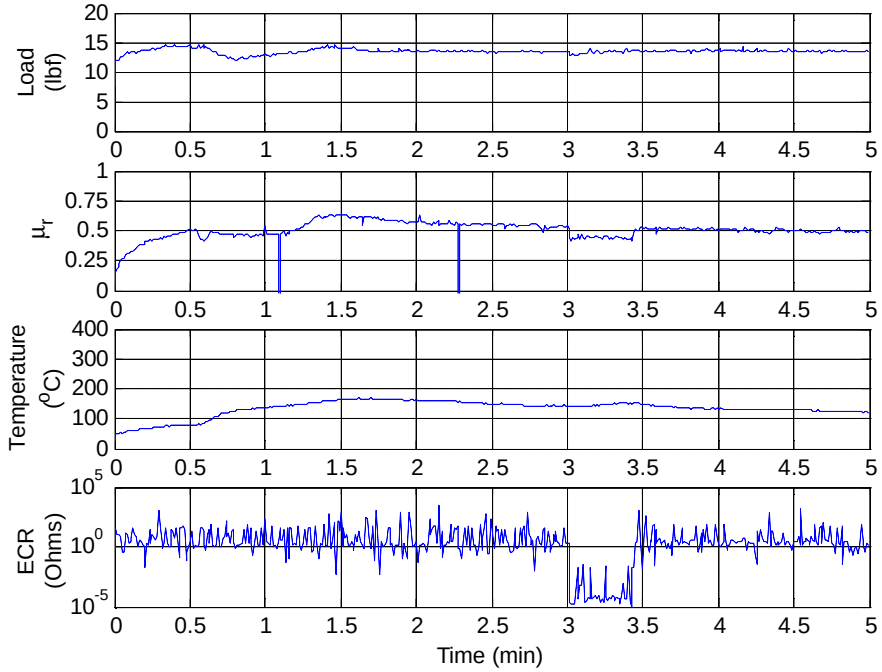

Figure 3.12 - R134a, 25 psi, 60°C

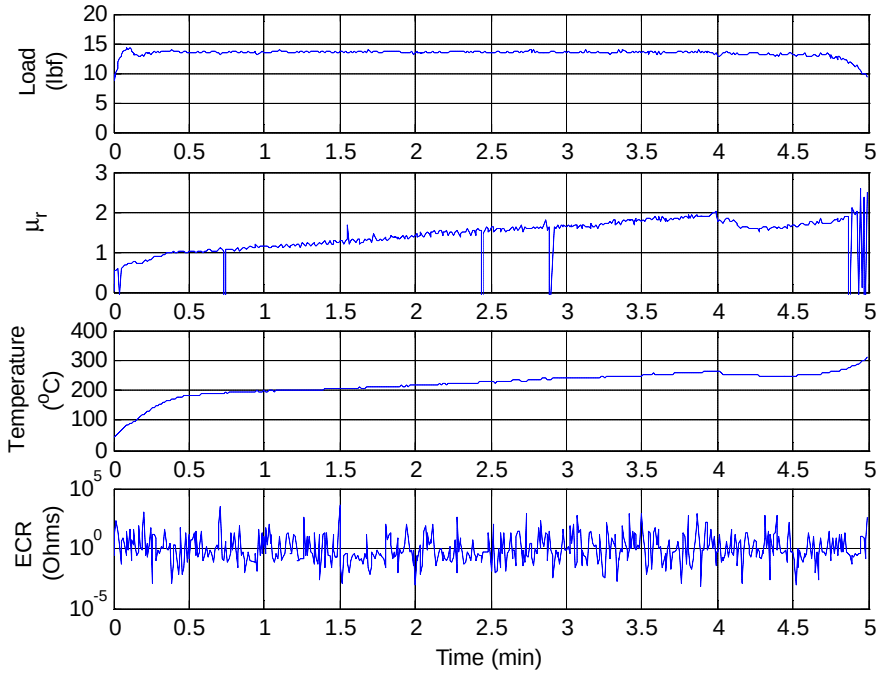

Figure 3.13 - Air, 60°C

The coefficient of friction in the case of CO_2 with a value of 0.5 is very similar to the one exhibited under the presence R134a. On the other hand, in the presence of air, the results are significantly different. The coefficient of friction starts out high at a value of about 1 and continuously increases to a value of 2 at the end of the test of 5 minutes. This can be seen in Figure 3.13. We may also note is that the near-contact temperature in the case of CO_2 is about the same as in the case of R134a taking a value of approximately 100°C. The contact temperature in the presence of air was unstable and increased from an initial value of 200°C to 300°C at the end of the test. From these experiments the positive effect of refrigerant can be seen.

Wear measurements for these experiments were taken. Theses are shown in Figure 3.14, for CO_2, R134a and air. They have been included in the same figure for direct comparison. As we can see the wear is higher in the case of air where the wear depth is approximately 4 μm whereas for CO_2 and R134a the wear depth is approximately 2μm. This is what one would have expected, since generally, wear increases with increasing coefficient of friction.

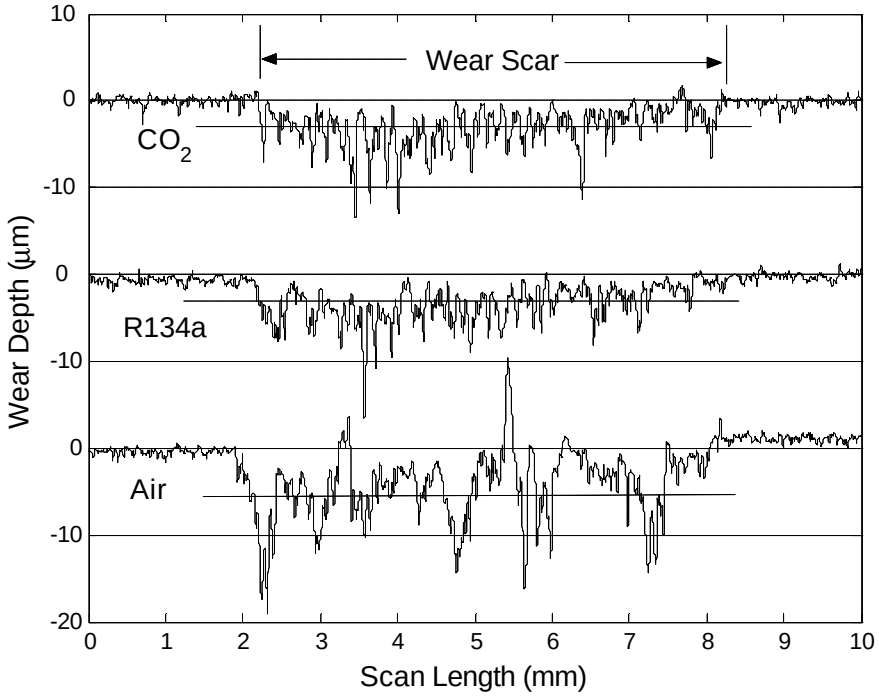

Figure 3.14 - Wear Measurement for CO_2, R134a and air, 50 psi, 60°C

Wear was also quantified in terms of the pins. The results for CO_2, R134a and air are shown in Table 3.1. The final weight of the pins tested in CO_2 and R134a environments is similar whereas the final weight of the pin tested in air decreased significantly.

A summary of the experimental conditions and the results obtained for CO_2, R134a and air compared under dry conditions is shown in Table 3.1.

Table 3.1 experimental conditions and results obtained for CO_2, R134a and air

Refrigerant		CO_2	R134a	Air
Chamber Pressure (psi)		50	25	14.5
Chamber Temperature (°C)		60	60	60
Load (lbf)		14	14	14
Linear Speed (m/s)		2.4	2.4	2.4
Pin weight (g)	Before	1.407	1.408	1.407
	After	1.395	1.393	1.330
Pin Wear (g)		0.012	0.015	0.077
Near-contact Temperature (°C)		90-130	100-150	200-300
Friction Coefficient		0.5	0.5	1-2
		Constant	Constant	Increasing

3.4 Type IV-Fully Submerged in PAG Lubricant

The issue of immiscibility was once again resolved by completely submerging the contacting surfaces in lubricant and simply pressurizing the chamber with refrigerant. So, once again we had known fixed thermodynamic conditions just like the Type I tests. That initiated Type IV experiments which are similar to Type I, but in the presence of lubricant. These experiments simulate ideal compressor conditions. Under these conditions, the

coefficient of friction remains very low and there is no detectable wear on the disks after the experiments. Very high loads and long time durations were needed in order to see minor wear or burnishing. The shoe-on-disk (Steel 52100 on Al 390-T6) geometry was used for these tests.

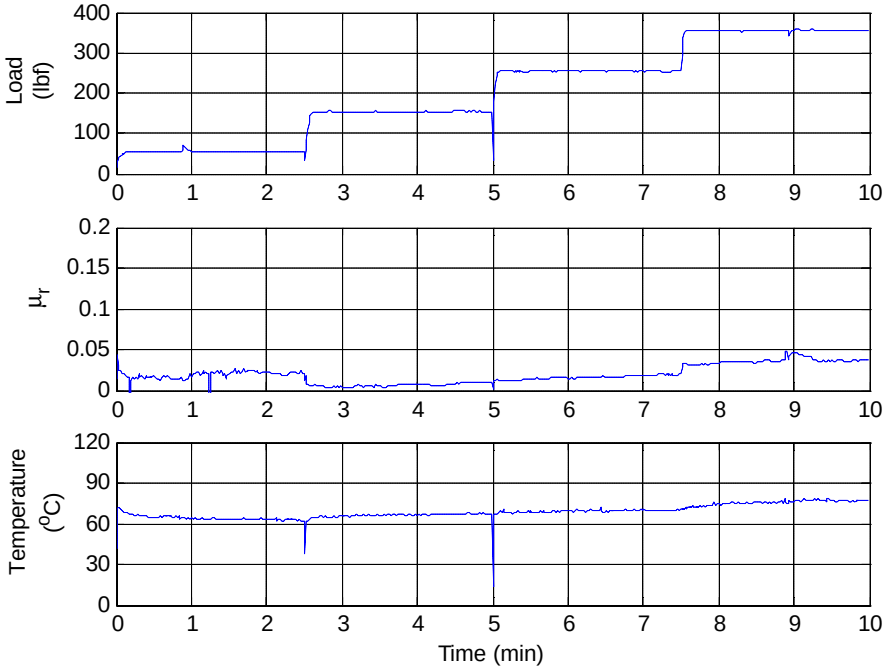

Figure 3.15 – Submerged Test in PAG lubricant in a CO_2 Environment for a Time Duration of 10 minutes

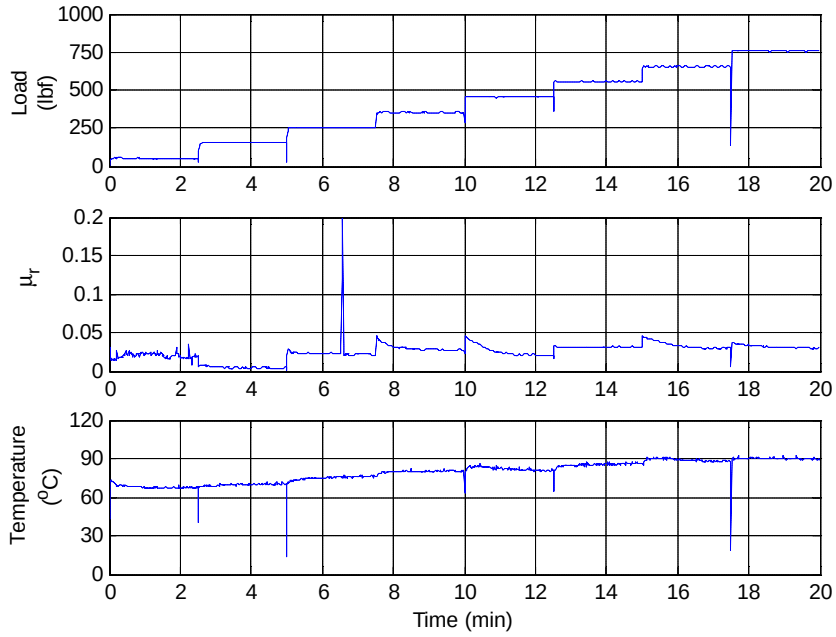

Figure 3.16 – Submerged Test in PAG lubricant in a CO_2 Environment for a Time Duration of 20 minutes

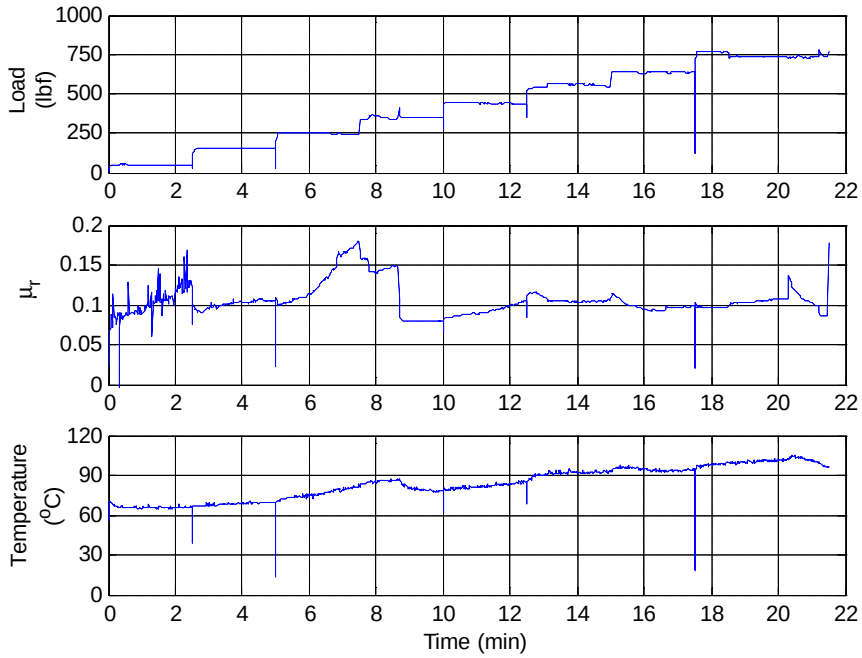

Figure 3.17 - Submerged Test in PAG Lubricant in a CO_2 Environment for a Time Duration of 22 minutes

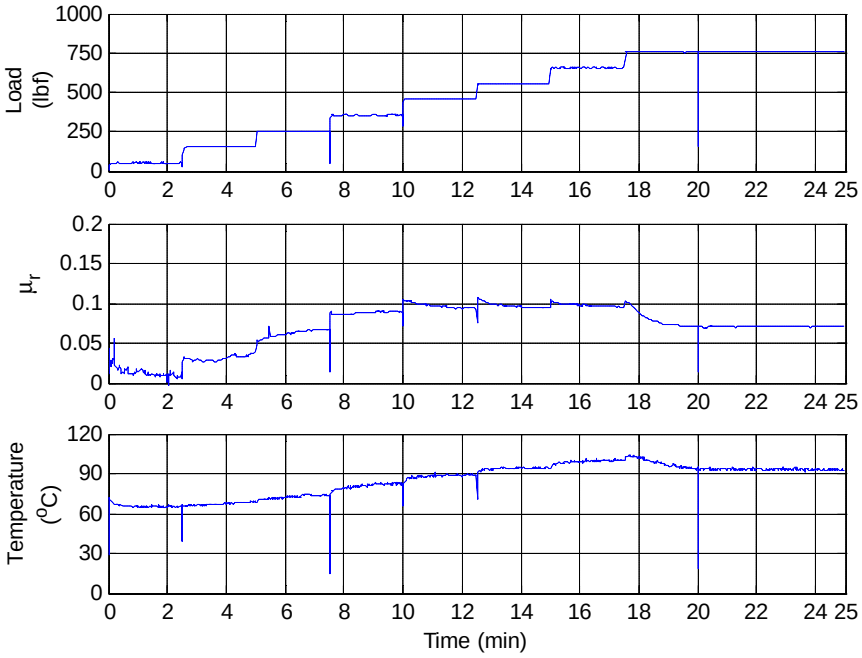

Figure 3.18 - Submerged Test in PAG Lubricant in a CO_2 Environment for a Time Duration of 25 minutes

It is our understanding that companies routinely perform tests under these conditions, where refrigerant is usually provided near the contact under atmospheric conditions using a “bubbling” method.

Several fully submerged tests were performed using PAG oil and CO_2. For each experiment, progressively higher normal loads were imposed for selected time durations. The time durations for these tests were 10 minutes, 20 minutes, 22 minutes, and 25 minutes. The results can be seen below on Figures 3.15 through 3.18.

Due to the fact that the specimens were fully submerged in PAG oil, both the coefficient of friction and the near-contact temperature have remained very low. These types of tests simulate ideal compressor conditions.

A microscope image for the sample tested for 22 minutes is shown in Figure 3.19. The image of this disk is similar to the images of the scuffing experiments that were analyzed by (Pergande, 2003). There is no significant wear and all disks after the tribological testing seem to undergo minute wear or burnishing.

Figure 3.19 - Microscope Image of Al390-T6 Disk: Sample C (t = 22 min)

No definite conclusions can be drawn from the series of the submerged tests. The reason for this is that actual scuffing time cannot be obtained due to the idealistic conditions of the contact being submerged in lubricant.

3.5 Type V-Direct Application of PAG Lubricant via Absorbing Medium

The idealistic case of Type IV tests led us to the development of Type V tests, which is the final type of experiments presented in this work. The idea behind the development was still the same as before with Type III. Resolve the issue of immiscibility, but create a more realistic environment for testing. The amount of oil had to be reduced and reasonably high loads would have to provide us with scuffing results that could be quantified. That was made possible by directly applying lubricant to the contact by means of an absorbing medium. Every time the disk rotated the contact was lubricated and the lubrication was in the mixed boundary and mixed regime, which indicated that there is a load, at which scuffing can occur. The cast iron pin-on-disk geometry was used for these tests.

3.5.1 Comparison of CO_2 with R134a

This is the most realistic case and we believe that the simplicity and the consistency in the results obtained can provide us with qualitative results for a comparative study, and the results seem to support that. The effect of using different refrigerant was examined once again but in the presence of PAG lubricant. CO_2 was compared to

R134a. As we can see from Figures 3.20 and 3.21, scuffing occurred right at 8 minutes for both refrigerants under the same conditions.

The friction is the same for both cases as well. It remained low taking a constant value of 0.1 for the duration of the test until scuffing at which point it increased dramatically.

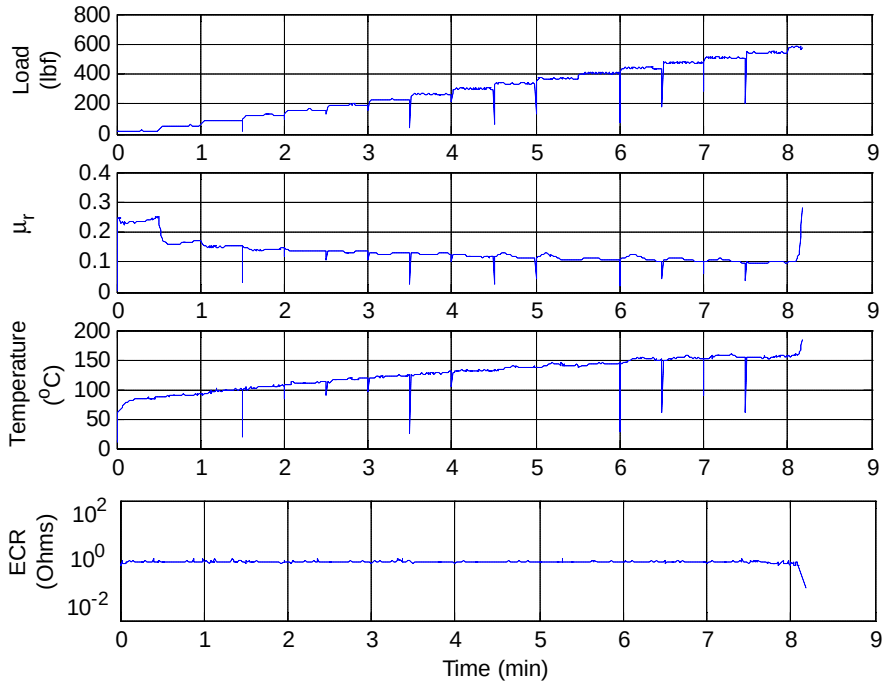

Figure 3.20 - CO_2, 200 psi, 120°C

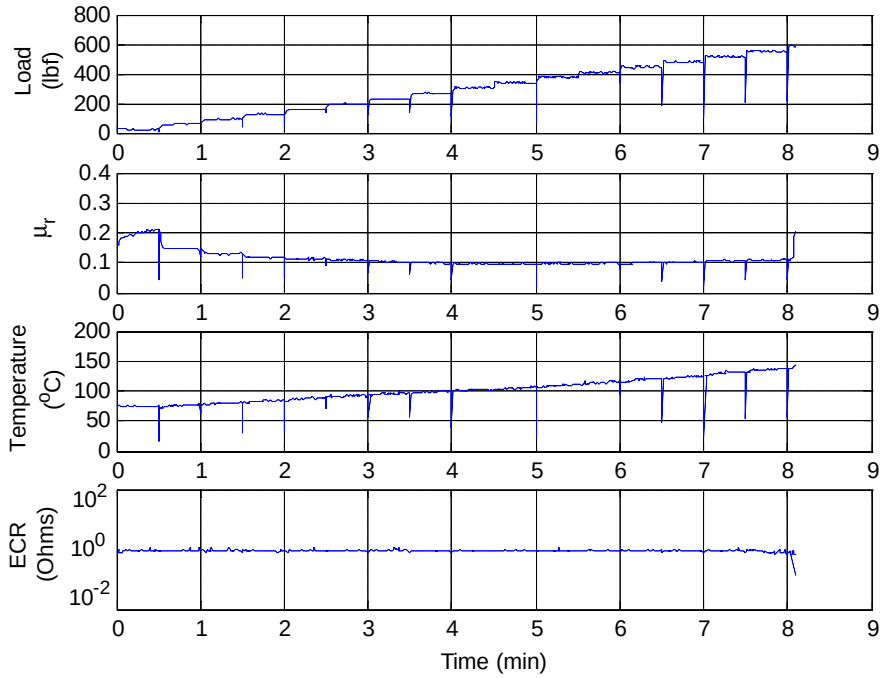

Figure 3.21 - R134a, 25 psi, 120°C

The near-contact temperature for both refrigerants has remained the same for the whole duration of the experiments. It always remained below 150°C, which occurred at the point of scuffing even though the chamber temperature was set to 120°C. The ECR values seem to indicate that the contact is in the boundary lubrication regime, which makes sense since there is a lubricant film between the contacting surfaces. One should notice that, as the lubricant film breaks right before 8 minutes the ECR drops. So, it appears that both refrigerants performed the same and that the scuffing time is not influenced by the presence of one refrigerant versus the other.

Wear measurements on the disks after the experiments seem to reinforce what was observed in the Type I test when CO_2 was compared to R134a. The wear measurements on the disk after the experiment are shown in Figure 3.22 for both CO_2 and R134a. We note that there is slightly less wear for R134a than there is in the case of CO_2, however, the difference between the two is minute and it is has to do with the fact that the CO_2 failed a second later than R134a, so more material was removed.

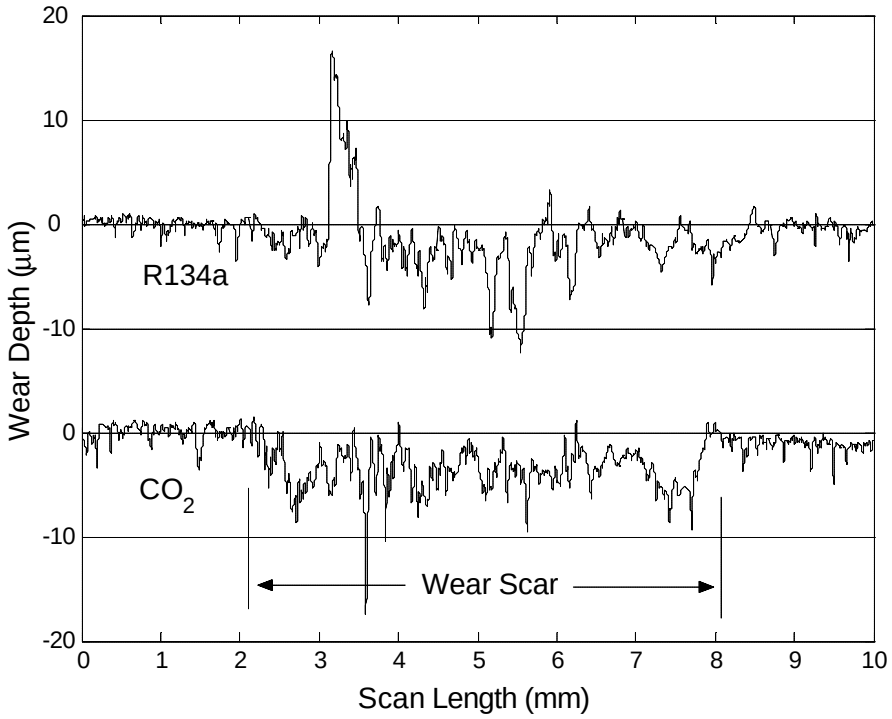

Figure 3.22 - Wear Measurement for CO_2 (200 psi, 120°C) and R134a (25 psi, 120°C)

From this type of test we note that the presence of lubricant seems to have a very strong effect that governs over the lubricative properties of the refrigerants. So, it appears that both refrigerants performed the same and that the scuffing time is not influenced by the presence of one refrigerant versus the other.

Chapter 4. Experimental Uncertainties and Techniques

4.1 Experimental Techniques

In this chapter, some of the problems encountered during this work have been summarized, which is intended to serve as a guide for experimental testing and emphasizes the things one should be looking after or avoid doing. Also some experimental techniques have been suggested to help making the experiments run smoothly while avoiding complications.

Many times during the setup of a specific type of test, decisions have to be made as to what the load should be for given environmental conditions so that the given geometry and the material could withstand the load. The way the load was selected was by numerous trials under a selected environmental condition. An important factor was also whether the load application should be constant or increased in a step-loading manner. If a standard wear test is preferred, then a constant load is applied. A step-loading test allows us to test to failure (scuffing).

When no lubricant is present the decision of what the load should is difficult since it has been observed that a material pair may scuff at very low loads. On the other hand, when lubricant is present, scuffing will only occur at very high loads. During this work two different material interfaces were studied, Al 390-T6 and cast iron. The shoe-on-disk geometry of Steel 52100 shoes on Al 390-T6 disks was used only under the Type IV-fully submerged in PAG lubricant tests. However, a great deal of experience has been gained by working with the pin-on-disk geometry of cast iron pins on cast iron disks through both lubricated and non-lubricated tests. Load selection for these are discussed in the sub-sections below.

4.1.1 Load Selection for Type I-Dry, Non-Lubricated Tests

Typically, under dry conditions, without the presence of lubricant, the load that can be sustained from the pin-on-disk geometry using different materials is very low. The materials tested during this work as previously mentioned were cast iron pins on cast iron disks, and Steel 52100 shoes on Al390-T6 disks. During this work it was realized that failure can occur within a couple of minutes or in some cases seconds even with constant loads around $20lb_f$. Figure 4.1 shows a test done on cast iron pin-on-disk that had a thin lubrite coating of 5-10μm.

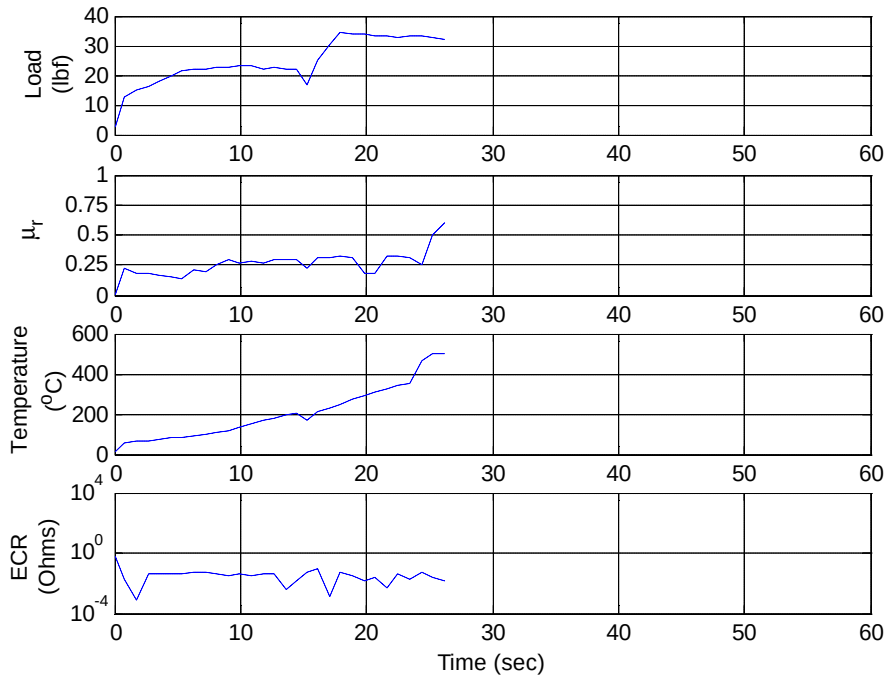

Figure 4.1 - Failure due to Increase in Load under Dry Conditions

As we can see, after the initial load of 20 lb_f is applied, the temperature starts increasing dramatically. After 15 seconds, the increase in the load to 35 lb_f causes the material to fail as we see from the rapid increase in friction and the very significant increase in temperature. Furthermore, the value of contact resistance being low indicates that there is significant asperity contact. Notice that the value of the coefficient of friction does not increase immediately after the step loading but approximately 10 seconds after the load increase. This is observed quite often if the current step load is neither high enough to cause failure right away nor low enough to be sustained for a longer period. Therefore, it was decided that for all the Type-I, dry experiments, non-lubricated tests under presence of CO_2 and R410a, a constant load of 17 lb_f is adequate. Such tests can be viewed as screening tests to assess the overall influence of a refrigerant on the tribological behavior of a specific interface.

4.1.2 Load Selection for Type V-Direct Application of PAG Lubricant

In the previous section we showed how the load was selected for a non-lubricated test. Unlike that type of test, which was done under a constant load, the direct application of lubricant test was done under a step load. The problem in this case was that any slight excess of lubricant makes it almost impossible to result in scuffing even at very high loads. Therefore, the parameter that was varied was the amount of oil. This was also something that was determined through numerous trials. One would think that it is possible to go to very high loads close to the machine's capability and cause scuffing. However, that may not be true since as it was realized only 50 mg of oil can be adequate to prevent scuffing and even excessive wear to loads up to 600 lb_f. The amount of 50 mg is the recommended amount in this case. That was applied with a syringe to a cloth as described in Section 2.5.7.

4.2 Pin Separation (HPT Low Load Capability)

It was previously mentioned that a constant load of 17 lb_f is adequate for the Type-I experiments. Part of the reason why it was decided that such load is adequate was that loads higher than 17 lb_f cause an almost immediate

failure. Another reason is that sometimes, when operating under low loads, usually around 10-15 lb_f, pin separation occurs at which the contact between the pin and the disk is lost and the test has to be stopped. This has been noticed several times when operating at very low loads. An example is shown in Figure 4.2 where pin separation occurred at approximately 3 minutes. One should keep in mind that operating at loads in this vicinity are very near the noise levels of the machine, for it was designed to operate at loads at least one order of magnitude higher. Therefore, one should avoid using loads less than 10 lb_f.

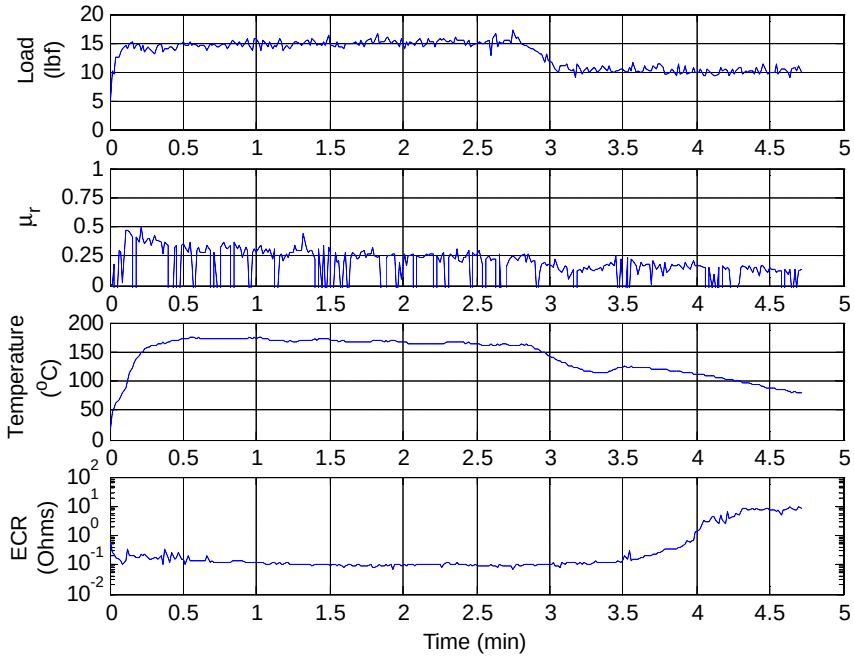

Figure 4.2 - Pin Separation as a Result of Low Load

4.3 Examples of Erratic Behavior due to Software Issue

Sometimes peculiar behavior can be observed in the data as a result of the machine's malfunction or by some error in operation. The most common examples one can come across when operating the HPT are software related.

In Figure 4.3 we observe an enormous increase in the contact load. Right when the contact is made the machine received a wrong signal that loads the specimen with full capacity. That was encountered once when the data acquisition card was malfunctioning and needed replacement. Even though the exact reason why that occurred is not known, it is believed that it was due to the card connector being plugged in backwards. One may notice that there are arrows on both the plug and the connector. The arrows should be aligned in order for the computer to properly function and the correct signals to be transmitted between the computer and the HPT panel.

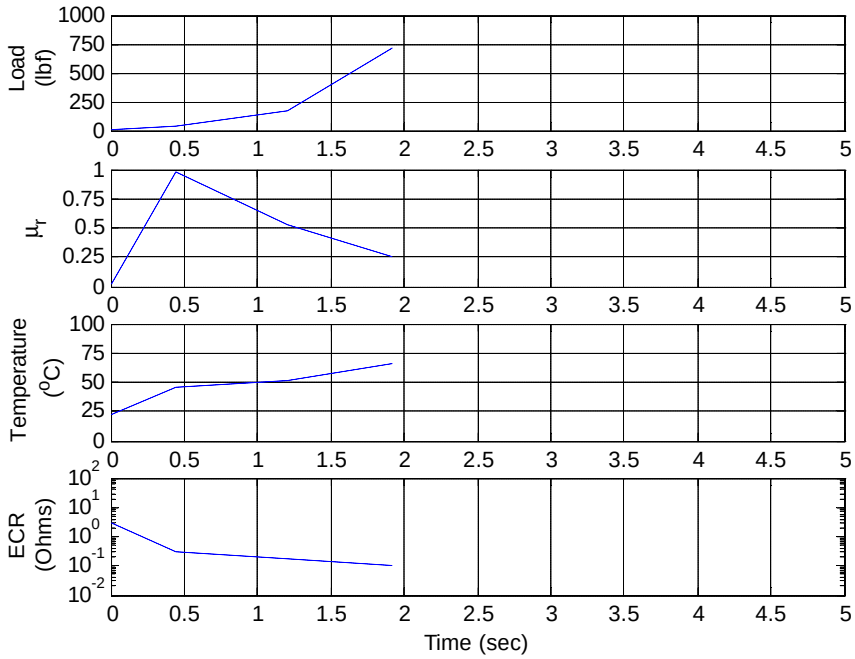

Figure 4.3 - Failure due to a Non-functioning Data Acquisition Board

4.4 Avoiding Condensation

Sometimes, one may wish to perform experiments at low temperatures. A common phenomenon that is encountered when that is the case is condensation. If for example we set the re-circulator chiller unit to 0°C, as one would have expected, condensation is evident in the fluid lines of the HPT as well as the spindle where the disk sample is mounted as the water vapor in the air condenses. By cooling down the specimen this way one can examine the effects of water in the contact. In order to avoid condensation, the chamber of the tribometer has to be closed, heated up to 100°C, evacuated and then cooled down to 0°C. In our results, it appears that the water has a positive effect, mostly in the temperature as it remains lower than in the case without the presence of water.

4.5 Repeatability of Results

The main concern with the results presented in Section 3.3.1 where the effects of pressure and temperature were examined was repeatability. Even though we tried to include representative data for all cases we feel it is necessary to mention that several of these tests were repeated due to lack of repeatability. A possible explanation for this is the inconsistency in the surface finish of the cast iron pins used for this series of tests. Theoretically that should not have a significant effect, but is possible that the test is initiated differently and consequently progressed differently giving variable results. Also, some of the gray cast iron disks used for tests had a PARCO® Lubrite No. 2 coating of 5-10 μm. The composition of this coating can be seen in Table A.3 in the Appendix. One needs to also keep in mind that the HPT was designed to operate at loads an order of magnitude higher. The pin is placed in a self-aligning holder so that motion is not restricted, but in order for precise alignment the load has to be relatively high, especially when the friction force is large. So, another possible explanation for variability is the low loads used for this type of tests.

The results presented in Section 3.3.2 and 3.5 on the other hand were quite repeatable. Once again the reason why in this case we were able to obtain repeatable results was probably the fact that the samples were prepared in a more consistent way and also for the direct application of lubricant via absorbing medium the loads used were significantly higher than before.

Chapter 5. Conclusions and Recommendations

5.1 Main Conclusions

CO_2 is thermodynamically much different than conventional refrigerants such as R134a. Thermodynamic properties cannot be ignored when tribological testing is performed. The previously developed method by Cusano and Stokes that has extensively been used in the past to test the performance of numerous material interfaces under the presence of refrigerants such as R134a cannot be used with CO_2 as a refrigerant due to immiscibility.

All of the 5 different types of tests presented in this research work were performed in order to better understand the behavior of CO_2 compared to other refrigerants. Due to the thermodynamic complexities involved in Types II and III and the discrepancies observed in some preliminary work during the Type III test we tried to isolate some of the thermodynamics, which initially led us to performing Type I and later on Type IV and V tests.

In this work we have presented a reliable way for testing under the presence of CO_2. Even though there was a limiting factor with our tester that was not designed for CO_2 testing, but for other conventional refrigerants, through a different approach and some modifications, we were able to establish a protocol for testing under the presence of CO_2. CO_2 was then compared to R134a. The previously encountered issue of miscibility under the setup developed by Cusano was overcome by supplying the lubricant separately from the refrigerant while the environment was pressurized with refrigerant. We were able to establish thermodynamically stable tests and we also test at extreme compressor conditions, both severe (dry) and ideal (fully submerged in lubricant). Furthermore, we examined the more realistic case of lubrication in the boundary and mixed regime.

From the experimental results of this study it is concluded that under the presence of PAG lubricant and the same environmental conditions, CO_2 and R134a performed very similarly. Furthermore, in the absence of lubricant, CO_2 performed very similar to R134a. From the submerged tests no definite conclusions can be drawn since due the idealistic condition scuffing was not observed. Finally, through this research work, the importance of the presence of oil was realized.

5.2 Future Work

Further investigation under higher pressures such as the ones encountered during transcritical operation for CO_2 is needed to compare it to R134a and it is proposed as future work.

In addition a more in depth study of parameters like the fluid retention index should be considered to get an understanding on how scuffing progresses under the conditions examined in this research work.

Bibliography

AMTI (1991), “High Pressure Tribometer”, Advanced Mechanical Technologies

ASHRAE (1969), “Thermodynamic Properties of Refrigerants”

Baek, J., Groll, E.A., Lawless, P.B., “Development of a Piston-Cylinder Expansion Device for the Transcritical Carbon Dioxide Cycle”, 2002 International Compressor Engineering Conference, Purdue University, West Lafayette, IN

Brown, J.S., Yana-Motta, S.F., Domaski, P.A. (2002), “Comparative Analysis of an Automotive Air Conditioning Systems Operating with CO_2 and R134a”, International Journal of Refrigeration, Vol. 25, pg. 19-32

Cavatorta, M.P. (1998), “Running-In and Scuffing in Aluminum/Steel Sliding Contacts”, Ph.D. Thesis, Politechnico di Torino

Cusano C., Stokes N. (1999), “Preliminary Results for the Scuffing Behavior of a CO_2/PAG Mixture”, ACRC Report # 157

Davis, B., Sheiretov, T.K., Cusano, C., “Tribological Evaluation of Contents Lubricated by Oil-Refrigerant Mixtures”, 1992 International Compressor Engineering Conference, Purdue University, W. Lafayette, IN pp. 477-487

Drees, D., Fahl, J., Hinrichs, J., “Effects of CO_2 on Lubricating Properties of Polyesters and Polyalkene Glycols”, Proceedings of the 13th International Colloquium Tribology, Lubricants, Materials and Lubrication Engineering, Technische Akademie Esslingen, January 15-17, 2002

Hagita, T., Makino, T., Horaguchi, N., Ukai, T. (2002), “Tribology in CO_2 Scroll Compressors”, Mitsubishi Heavy Industries, Ltd., Technical Review Vol.39 No. 1

Hsinheng, L., Lilje, K.C., Watson, M.C., “Field and Laboratory Evaluations of Lubricants for CO_2 Refrigeration”, 2002 International Compressor Engineering Conference, Purdue University, West Lafayette, IN

Jonsson, U. (1998), “Elastohydrodynamic Lubrication Rheology in Refrigeration Compressors”, Doctoral Thesis, Institutionen for Maskinteknik

Lorentzen, G. (1995), “The Use of Natural Refrigerants: A Complete Solution to the CFC/HCFC predicament”, International Journal of Refrigeration, Vol. 18, No. 3, pp 190-197

Ohkawa, T., Kumakura, E., Higashi, H., Sakitani, K., “Development of Hermetic Swing Compressors for CO_2 Refrigerant”, Daikin Air Conditioning R&D Laboratory Ltd., 2002 International Compressor Engineering Conference, Purdue University, West Lafayette, IN

Matlock, P.L., Brown, W.L., Clinton, N.A. (1999) “Polyalkylene Glycols in Synthetic Lubricants and High Performance Functional Fluids”, (Rudnick, L.R., and Shubkin, R.L., ed.), Marcel Dekker, Inc., p159

Patel, J. J. (2000), “Investigation of the Scuffing Mechanism Under Starved Lubrication Conditions Using Macro, Meso, Micro and Nano Analytical Techniques”, M.S. Thesis, University of Illinois at Urbana-Champaign

Pergande, S. R., Polycarpou, A. A. (2003), “Nanomechanical Properties of Aluminum 390-T6 Rough Surfaces Undergoing Tribological Testing”

Pettersen, J., “Experimental Results of Carbon Dioxide in Compression Systems” AHRAE/NIST Refrigerants Conference-Refrigerants for the 21st Century, October 1997

Randles, S.J. (1999), “Esters in Synthetic Lubricants and High-Performance Functional Fluids”, (Rudnick, L.R., and Shubkin, R.L., ed.), Marcel Dekker, Inc., p63

Sheiretov, T. K., Yoon, H.K., Cusano, C. (1998), “Scuffing under Dry Sliding Conditions”. Part 1: Experimental Studies, STLE Tribology Transactions, Vol. 41 (4), pp. 435-446

Suss, J., “Low Capacity Hermetic Type Compressor for Transcritical CO_2 Applications”, 2002 International Compressor Engineering Conference, Purdue University, West Lafayette, IN

Yoon, H.K. (1999), “Scuffing Under Starved Lubrication Conditions”, PhD. Thesis, University of Illinois at Urbana-Champaign

Appendix A

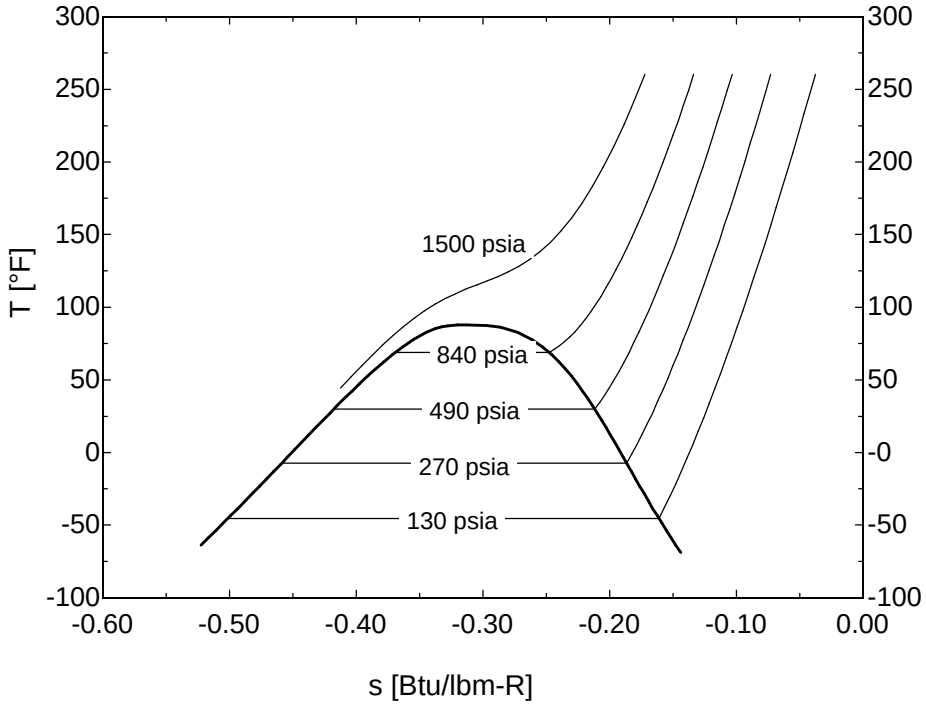

Figure A.1 - Temperature-Entropy Diagram for CO_2

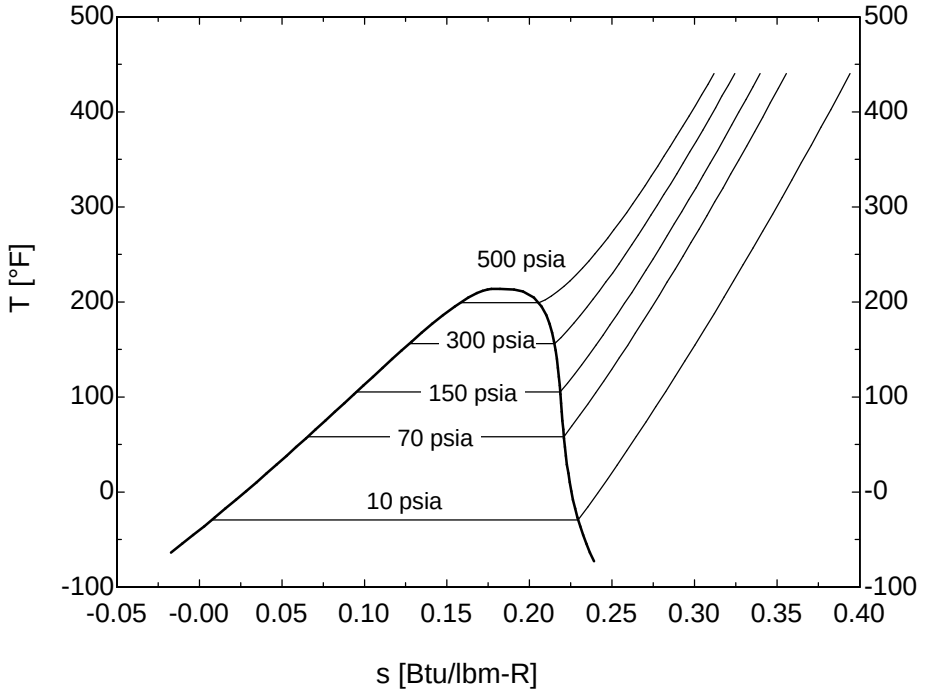

Figure A.2 - Temperature-Entropy Diagram for R134a

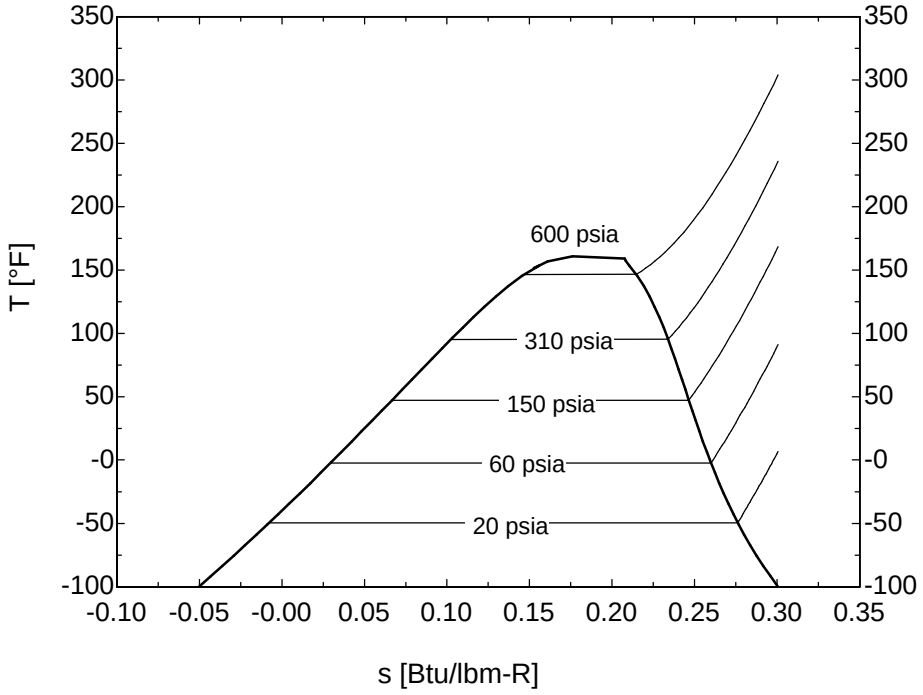

Figure A.3 - Temperature-Entropy Diagram for R410a

Table A.1 - Properties of Carbon Dioxide (ASHRAE, 1969)

Chemical Formula	CO_2
Molecular Weight	44.011
Normal Sublimation Temperature at Atmospheric Pressure, °F	-109.21
Triple Point Temperature (at 75.35 psi), °F	-69.88
Critical Temperature, °F	87.87
Critical Pressure, psi	1069.96
Critical Density, lb/ft^3	29.21
Density of Liquid at 86 °F, lb/ft^3	37.3
Specific Volume of Saturated Vapor at 5 .F, lb/ft^3	0.266
Specific Heat of Liquid at 86°F, Btu/(lb °F)	2.5
Specific Heat Ratio (C_p/C_v) of Vapor at 86°F and 1atm	1.3
Thermal Conductivity, (Btu)(ft)/(ft^2 hr °F):	
Saturated Liquid at 5°F	0.067
Saturated Liquid at 86°F	0.041
Vapor at Saturation Pressure at 5°F	0.0139
Vapor at 1atm at 86°F	0.0169
Viscosity, Centipoises:	
Saturated Liquid at 5°F	0.13
Saturated Liquid at 86°F	0.065
Vapor at Saturation Pressure at 5°F	0.013
Vapor at 1 atm at 86°F	0.015
Relative Dielectric Strength of Vapor at ambient temperature and 1 atm (Nitrogen=1)	0.88
Color	Clear and water white
Flammability	Nonflammable
Toxicity, Underwriters' Laboratories Classification	Group 5a
Other name	R744

Table A.2 - Properties of R12 (ASHRAE, 1969)

Chemical Formula	CCl_2F_2
Molecular Weight	120.93
Boiling Temperature at Atmospheric Pressure, °F	-21.6
Freezing Temperature at Atmospheric Pressure, °F	-252
Critical Temperature, °F	233.6
Critical Pressure, psi	597
Critical Density, lb/ft^3	34.84
Density of Liquid at 86 °F, lb/ft^3	80.67
Specific Volume of Saturated Vapor at 5 .F, lb/ft^3	1.458
Specific Heat of Liquid at 86°F, Btu/(lb °F)	0.235
Specific Heat Ratio (C_p/C_v) of Vapor at 86°F and 1atm	1.139
Thermal Conductivity, (Btu)(ft)/(ft^2 hr °F):	
Saturated Liquid at 5°F	0.052
Saturated Liquid at 86°F	0.040
Vapor at Saturation Pressure at 5°F	0.0047
Vapor at 1atm at 86°F	0.0059
Viscosity, Centipoises:	
Saturated Liquid at 5°F	0.335
Saturated Liquid at 86°F	0.254
Vapor at Saturation Pressure at 5°F	0.0108
Vapor at 1 atm at 86°F	0.0127
Relative Dielectric Strength of Vapor at ambient temperature and 1 atm (Nitrogen=1)	2.4
Color	Clear and water white
Odor	Faint ethereal odor
Flammability	Nonflammable
Toxicity, Underwriters' Laboratories Classification	Group 6
Other name	Dichlorodifluoromethane

MATERIAL SAFETY DATA SHEET

1. CHEMICAL PRODUCT AND COMPANY INFORMATION

Product Trade Name: PARCO® LUBRITE 2

HENKEL CORPORATION, PARKER AMCHEM

32100 Stephenson Highway

Madison Height, MI 48071

Telephone number: (810) 583-9300

Emergency Number: (800) 424-9300

2. COMPOSITIOM INFORMATION

Table A.3 - Composition Information for PARCO® LUBRITE 2

COMPONENT	PERCENT
Phosphoric Acid	1-10
Nitric Acid	1-10
Nickel Nitrate	<1
Manganese Dihydrogen Phosphate	20-40